

INTERNATIONAL FORENSIC SCIENCE
AND INVESTIGATION SERIES

Second Edition

Forensic Investigation of Explosions



Edited by
Alexander Beveridge

Second Edition

Forensic Investigation of Explosions

INTERNATIONAL FORENSIC SCIENCE AND INVESTIGATION SERIES

Series Editor: Max Houck

**Scientific Examination of Documents:
methods and techniques, 2nd edition**

D Ellen

ISBN 9780748405800

1997

Forensic Examination of Human Hair

J Robertson

ISBN 9780748405671

1999

**Forensic Examination of Fibres,
2nd edition**

J Robertson and M Grieve

ISBN 9780748408160

1999

**Forensic Examination of Glass and Paint:
analysis and interpretation**

B Caddy

ISBN 9780748405794

2001

Forensic Speaker Identification

P Rose

ISBN 9780415271827

2002

Bitemark Evidence

B J Dorion

ISBN 9780824754143

2004

**The Practice of Crime Scene
Investigation**

J Horswell

ISBN 9780748406098

2004

Fire Investigation

N Nic Daéid

ISBN 9780415248914

2004

**Fingerprints and Other Ridge Skin
Impressions**

*C Champod, C J Lennard, P Margot,
and M Stoilovic*

ISBN 9780415271752

2004

**Firearms, the Law, and Forensic Ballistics,
Second Edition**

Tom Warlow

ISBN 9780415316019

2004

Forensic Computer Crime Investigation

Thomas A Johnson

ISBN 9780824724351

2005

**Analytical and Practical Aspects of
Drug Testing in Hair**

Pascal Kintz

ISBN 9780849364501

2006

**Nonhuman DNA Typing: theory and
casework applications**

Heather M Coyle

ISBN 9780824725938

2007

**Chemical Analysis of Firearms,
Ammunition, and Gunshot Residue**

James Smyth Wallace

ISBN 9781420069662

2008

Forensic Science in Wildlife Investigations

Adrian Linacre

ISBN 9780849304101

2009

**Scientific Method: applications in failure
investigation and forensic science**

Randall K Noon

ISBN 9781420092806

2009

Forensic Epidemiology

Steven A Koehler and Peggy A Brown

ISBN 9781420063271

2009

Ethics and the Practice of Forensic Science

Robin T Bowen

ISBN 9781420088939

2009

**Introduction to Data Analysis with R for
Forensic Scientists**

James Michael Curran

ISBN: 9781420088267

2010

**Forensic Investigation of Explosions,
Second Edition**

A Beveridge

ISBN 9781420087253

2011

INTERNATIONAL FORENSIC SCIENCE
AND INVESTIGATION SERIES

Second Edition

Forensic Investigation of Explosions

Edited by

Alexander Beveridge



CRC Press

Taylor & Francis Group

Boca Raton London New York

CRC Press is an imprint of the
Taylor & Francis Group, an **informa** business

CRC Press
Taylor & Francis Group
6000 Broken Sound Parkway NW, Suite 300
Boca Raton, FL 33487-2742

© 2012 by Taylor & Francis Group, LLC
CRC Press is an imprint of Taylor & Francis Group, an Informa business

No claim to original U.S. Government works
Version Date: 20111010

International Standard Book Number-13: 978-1-4665-0394-6 (eBook - PDF)

This book contains information obtained from authentic and highly regarded sources. Reasonable efforts have been made to publish reliable data and information, but the author and publisher cannot assume responsibility for the validity of all materials or the consequences of their use. The authors and publishers have attempted to trace the copyright holders of all material reproduced in this publication and apologize to copyright holders if permission to publish in this form has not been obtained. If any copyright material has not been acknowledged please write and let us know so we may rectify in any future reprint.

Except as permitted under U.S. Copyright Law, no part of this book may be reprinted, reproduced, transmitted, or utilized in any form by any electronic, mechanical, or other means, now known or hereafter invented, including photocopying, microfilming, and recording, or in any information storage or retrieval system, without written permission from the publishers.

For permission to photocopy or use material electronically from this work, please access www.copyright.com (<http://www.copyright.com/>) or contact the Copyright Clearance Center, Inc. (CCC), 222 Rosewood Drive, Danvers, MA 01923, 978-750-8400. CCC is a not-for-profit organization that provides licenses and registration for a variety of users. For organizations that have been granted a photocopy license by the CCC, a separate system of payment has been arranged.

Trademark Notice: Product or corporate names may be trademarks or registered trademarks, and are used only for identification and explanation without intent to infringe.

Visit the Taylor & Francis Web site at
<http://www.taylorandfrancis.com>

and the CRC Press Web site at
<http://www.crcpress.com>

To everyone involved in the detection of explosives, the prevention of explosions, the forensic investigation of explosions, and the justice system. Your expertise and dedication make your society a safer and better place.

Table of Contents

List of Figures	xi
Series Editor's Note	xxvii
Preface	xxix
Contributors	xxxix
Editor	xxxvii
1 The History, Development, and Characteristics of Explosives and Propellants	1
ROBERT B. HOPLER	
2 Physics of Explosion Hazards	19
BIBHU MOHANTY	
3 Detection of Hidden Explosives: New Challenges and Progress (1998–2009)	53
SUSAN HALLOWELL, RICHARD LAREAU, RONALD KRAUSS, CURTIS BELL, JOSHUA RUBINSTEIN, POLLY GONGWER, PAMELA BERESFORD, AND JAMES C. WEATHERALL	
4 General Protocols at the Scene of an Explosion	79
JEAN-YVES VERMETTE	
5 Recovery of Material from the Scene of an Explosion and Its Subsequent Forensic Laboratory Examination—A Team Approach	119
RICHARD A. STROBEL	
6 The Management of Casework within the United Kingdom Forensic Explosives Laboratory	159
SHARON BROOME AND CLIFFORD TODD	
7 Aircraft Explosive Sabotage Investigation	197
JOHN H. GARSTANG	

8	Evidence of Explosive Damage to Materials and Structures in Air Crash Investigations	303
	MAURICE BAKER, JOHN WINN, STEVE HARRIS, AND NIGEL HARRISON	
9	Investigation of Gas Phase Explosions in Buildings	349
	CHRISTOPHER D. FOSTER	
10	Vehicle-Borne Improvised Explosive Devices: Collection, Analysis, and Presentation of Evidence	405
	DONALD J. SACHTLEBEN	
11	Investigation of Pipe Bombs	429
	EDWARD C. BENDER AND ALEXANDER D. BEVERIDGE	
12	Improvised Explosives Characteristics, Detection, and Analysis	493
	KIRK YEAGER	
13	Quality and the Trace Detection and Identification of Organic High Explosives	539
	SEAN DOYLE	
14	Chromatography of Explosives	585
	BRUCE R. McCORD, INGE CORBIN, AND EDWARD C. BENDER	
15	Analysis of Explosives by Mass Spectrometry	621
	TSIPPY TAMIRI AND SHMUEL ZITRIN	
16	Analysis of Explosives by Infrared Spectrometry	671
	SHMUEL ZITRIN AND TSIPPY TAMIRI	
17	Portable Explosive Detection Instruments	691
	SARAH BENSON, NAOMI SPEERS, AND VINCENT OTIENO-ALEGO	
18	The Significance of Analytical Results in Explosives Investigation	725
	GERARD T. MURRAY	

19	Forensic Pathology of Explosive Injury	741
	INDIRA KITULWATTE AND MICHAEL S. POLLANEN	
20	Presentation of Explosive Casework Evidence	757
	JAMES W. JARDINE	

List of Figures

Figure 1.1	A family of explosives based on various monosubstitutions of a single hydrogen in 1,3,5 trinitrobenzene.	5
Figure 1.2	Structural formula of TNT.	6
Figure 1.3	Structural formula of PETN.	6
Figure 1.4	Structural formula of RDX.	7
Figure 1.5	Structural formula of HMX.	7
Figure 1.6	Structural formula of nitroglycerin.	9
Figure 1.7	Structural formula for TATP.	15
Figure 1.8	Structural formula for HMTD.	15
Figure 2.1	Chemical composition of typical molecular explosives.	22
Figure 2.2	Simplified structure of detonation reaction in an explosive mixture.	25
Figure 2.3	Energy distribution (schematic) in an explosion event as a function of time.	28
Figure 2.4	(a) Idealized propagation and decay of the shock wave from an explosion at increasing distances; (b) a typical shock pressure profile; (c) a measured shock profile from a small near-surface ANFO charge 6.4 kg (14 lb) at a distance of 2.1 m (7 ft) from the source.	30
Figure 2.5	Shock pressure profile from a free-air explosion and the associated dynamic pressure at a fixed distance from the explosion.	31
Figure 2.6	Formation of the triple point and Mach stem upon reflection of a shock wave.	32
Figure 2.7	Shock wave parameters (positive phase only) for a free-air spherical TNT explosion at sea level.	34
Figure 2.8	Changes in shock wave parameters due to change in shape of the explosive source for Composition B.	35
Figure 2.9	Gurney energy relations for calculation of fragment velocity for simple geometries.	41
Figure 2.10	An example of blast load calculation on the front wall of a box-like structure (pressure and time in arbitrary units).	44

Figure 2.11	Cubicle configuration and design parameters for calculation of impulse load for an internal explosion.	44
Figure 2.12	Parameters defining pressure design ranges.	45
Figure 2.13	Typical construction of reinforced concrete members for blast-resistant structures.	47
Figure 2.14	Pressure and impulse for lung damage due to a blast wave.	48
Figure 3.1	Three fundamental parameters for a basic explosives detection system.	59
Figure 3.2	Relative technology challenge in detecting bulk explosives.	60
Figure 3.3	Megavolt X-ray system for large-vehicle screening.	61
Figure 3.4	Z-backscatter imager.	62
Figure 3.5	Electromagnetic imaging systems use the part of the electromagnetic spectrum between radio and visible light.	63
Figure 3.6	The calculated difference in the millimeter intensity of an explosive and simulant material based on the matching of dielectric properties.	63
Figure 3.7	Solid line: The electromagnetic signal inside of an enclosed metallic cavity shows a resonant response at 240 MHz. Dashed line: A bottle of water inside the cavity shifts the resonant response to 235 MHz.	65
Figure 3.8	Canine responses to variants of TNT.	70
Figure 4.1	Motive, means, and opportunity.	81
Figure 4.2	A basic electrical circuit.	85
Figure 4.3	Aide-memoire for first responders, “CHALET.”	89
Figure 4.4	Aide-memoire for first responders, “SCENE.”	89
Figure 4.5	Chronology of investigative activities.	90
Figure 4.6	Detonation of dynamite in a baggage container.	92
Figure 4.7	Sequential development (a to b to c) of a fireball and debris produced by a charge of plastic explosive.	92
Figure 4.8	A natural gas explosion in a house.	93
Figure 4.9	The aftermath of a natural gas explosion in a house—the basement.	93
Figure 4.10	Simulated suicide bombing in a bus.	93
Figure 4.11	Properly attired members of a team entering a post-blast scene.	98
Figure 4.12	Incorrect attire and procedures for measurement of a bomb crater: contamination issues.	99
Figure 4.13	Anvil Roaming Emergency Communications Network (RECoN Pack).	100
Figure 4.14	3D laser scanning equipment.	102

Figure 4.15	Cross-section of the crater produced by the test explosion of a vehicle-borne IED.	103
Figure 4.16	Orthochromatic view of the scene of the test explosion of a vehicle-borne IED.	103
Figure 4.17	Chromatic view of the scene of the test explosion of a vehicle-borne IED.	103
Figure 4.18	Explosion scene perimeter.	104
Figure 4.19	Building plans can greatly assist investigators at a scene to get their bearings.	106
Figure 4.20	A test explosion in a train.	109
Figure 4.21	Initial observation of a train bombing.	109
Figure 4.22	A grid system surrounding a bombed car.	110
Figure 4.23	Narita Airport, Japan, bomb scene 1985.	111
Figure 4.24	Plan view of the Narita Airport bomb scene.	111
Figure 4.25	Seat of the Narita Airport explosion.	111
Figure 4.26	Recording and photographing individual exhibits, Narita Airport bomb scene.	112
Figure 4.27	Typical search patterns.	113
Figure 4.28	Use of an explosives detection dog.	114
Figure 4.29	Taking control samples from the scene of a seated explosion.	114
Figure 6.1	Equipment for drying and sifting debris.	163
Figure 6.2	Portable sifter as deployed by the Metropolitan Police to incidents in London, July 2005.	166
Figure 6.3	Train carriage wrapped ahead of transfer to the examination facility.	169
Figure 6.4	Cartridge case test results.	178
Figure 6.5	Set up for large-scale explosive tests of hydrogen peroxide mixtures.	183
Figure 6.6	Experimental set up for the TATP hydrogen peroxide/ flour firing trials.	184
Figure 6.7	Experimental setup for large-scale gap tests.	184
Figure 7.1	Mobile CBRN hazardous materials response trailer.	205
Figure 7.2	GIS display of the Flight SR111 occurrence site showing colored search zones along the coastline, and search lanes on the surface of the Atlantic Ocean.	215
Figure 7.3	VisionMap A3 digital mapping system installed in a belly camera port of an Ofec PA-31T survey aircraft.	223

Figure 7.4	VisionMap A3 orthophoto example produced with a 12 cm (5 in) GSD from a flight altitude of 12,000 ft (3656 m).	223
Figure 7.5	Side view of the portable ICAROS digital mapping system installed in a Cessna 172 aircraft, showing the sensor unit (inset) deployed in flight.	224
Figure 7.6	CQ-10A parafoil SnowGoose UAV being launched from the back of a HMMWV on a dirt road.	225
Figure 7.7	Oblique view of a C2SM robotic platform showing some of the major components.	227
Figure 7.8	Illustration showing the creation of a 3D stereo X-ray pair by taking two separate images.	228
Figure 7.9	Cropped vertical air photograph taken by NOAA of the World Trade Center on September 23, 2001, from an altitude of 3300 ft.	230
Figure 7.10	Rendered image from a 3D computer model produced by the U.S. Army Joint Precision Strike Demonstration team from LiDAR data collected by NOAA flights over the World Trade Center on September 27, 2001.	230
Figure 7.11	Side view of a mobile Titan LiDAR system mounted on a hydraulic hoist in road-rail truck and on the belly of a Robinson R44 helicopter.	232
Figure 7.12	Point cloud image of B727 aircraft created during an IED exercise by a Mobile Titan® LiDAR system mounted in the back of a pickup truck.	232
Figure 7.13	RADARSAT-1 SAR image showing oil slicks that formed in the Atlantic Ocean during a salvage operation.	234
Figure 7.14	Environment Canada DC-3 LEAF video image showing the location of a confirmed Jet A fuel hit on land.	234
Figure 7.15	Composite image showing insets of a S3900 and S5900 towfish overlaid on a side-scan sonar display.	237
Figure 7.16	Oblique view of the novel one-person Atmospheric Diving System (ADS) HARDSUIT™ Quantum.	240
Figure 7.17	The small two-man portable REMUS-100 AUV is capable of being launched and recovered by hand.	243
Figure 7.18	View of the Arctic Explorer AUV being deployed through an Arctic ice hole.	244
Figure 7.19	Side view of a mid-depth configured ROPOS ROV being deployed by a LARS crane.	245
Figure 7.20	Two ROPOS force feedback manipulators recover a desktop computer from a wreck in the Pacific Ocean at a depth of 1400 ft or 426 m.	246

Figure 7.21	General view of a ROPOS control room installed onboard a ship.	247
Figure 7.22	Composite image showing the disassembly of a DFDR and an analogue CVR recovered from the Flight SR111 wreckage.	253
Figure 7.23	Video frame from a flight recorder playback animation showing optional cockpit instrument displays below a chase plane view.	254
Figure 7.24	Computer rendition of a 3D trajectory analysis for a sequential in-flight breakup.	256
Figure 7.25	Exterior view of the post-blast longitudinal fracture created in the prepressurized fuselage of a B727 aircraft following the detonation of an IED in the forward cargo hold.	258
Figure 7.26	Interior view of the cargo hold showing crushed and broken frames near the center of the rupture.	258
Figure 7.27	Digital image correlation plot showing the formation of a blister deformation pattern in the exterior skin of a B727 aircraft following the detonation of an IED in the aft cargo hold.	259
Figure 7.28	Exterior view of a petaled hole created in the fuselage skin of an unpressurized B747 aircraft following the detonation of a high explosive IED in a ULD.	260
Figure 7.29	Composite view showing the concentration of staining and microcraters with some gas wash near the tip of a curl from a petaled hole in an aircraft fuselage.	261
Figure 7.30	Composite image showing 3D CAD models of the B747 aircraft, occupants, and cargo.	264
Figure 7.31	Composite image showing color-coded, generic, 3D anatomical body models used to depict autopsy and toxicology information for victim injury pattern analyses.	265
Figure 7.32	Oblique view showing the 3D CAD model of the forward section of the Flight SR111 aircraft.	266
Figure 7.33	General view of a page from a freeze-dried document showing the legibility of the entries after treatment.	268
Figure 7.34	General view of a questioned document showing the faded and partially obliterated “13A. Tire pressure—check” area of interest, situated to the right of the word “Main,” underlined and numbered from 1 to 8 inclusive.	269
Figure 7.35	Composite, close-up views of the same area of interest in Figure 7.34 showing two different VSC spectral returns.	270
Figure 7.36	General view of a burnt, water-soaked document that was frozen, freeze-dried and Parylene coated.	271

Figure 8.1	Selection of fragments showing typical shapes and sizes of fragments originating from explosions.	313
Figure 8.2	Selection of typical rolled edges.	314
Figure 8.3	A typical example of gas wash on an aluminum alloy fragment.	314
Figure 8.4	Impact crater or pit (sectional view).	315
Figure 8.5	Typical impact craters.	315
Figure 8.6	Secondary fragment impact sites forming halo around the principal fragment impact site.	316
Figure 8.7	Crater almost camouflaged by accumulated debris before and after cleaning.	316
Figure 8.8	Two examples of melt structures observed in the bottom of craters and on rolled edges, shown at different magnifications.	317
Figure 8.9	An experimental trial to illustrate the explosive cladding effect: a copper witness plate with aluminum deposited within the explosively formed craters.	318
Figure 8.10	Explosive flash melting on nylon 6-6.	319
Figure 8.11	Globularizing of fiber ends in nylon 6-6.	320
Figure 8.12	Micrograph of a wool-nylon mixture showing charring of wool-fiber ends and globularization of the nylon fibers.	320
Figure 8.13	Globularizing of fiber ends resulting from high-velocity fragment penetration.	320
Figure 8.14	Torn black holdall bag recovered from Lauda-Air 767 in Thailand in 1991.	321
Figure 8.15	Extended swelling from fiber ends, found on holdall bag.	321
Figure 8.16	Doll's dress material, interpenetration, and the fusing of pink fabric.	322
Figure 8.17	Examples of crystal twinning, adiabatic shear, and microrecrystallization.	323
Figure 8.18	Deformed grains in thin sheet metal—the "orange peel" effect.	324
Figure 8.19	Pitting corrosion in magnesium alloy.	325
Figure 8.20	Stereo view of corrosion pitting in magnesium alloy from overhead trunking.	326
Figure 8.21	Overlapping corrosion pits in stainless steel.	327
Figure 8.22	Crack formation in the aft fuselage of a pressurized Boeing 747 approximately 1/3 sec after the internal detonation of an explosive charge.	328

Figure 8.23	The trial aircraft after testing, showing a large panel of the aft fuselage side intact but creased with vertical cracks forward and aft of the longitudinal crack.	329
Figure 8.24	Air India wreckage trail plot grouped by original position on the aircraft.	330
Figure 8.25	Reflected impulse plotted against stand-off distance for increasing amounts of high explosive.	331
Figure 8.26	Pam Am 103 reconstruction.	332
Figure 8.27	Section of the Air India window belt as found on the sea bed.	332
Figure 8.28	Photograph showing part of the Air India Boeing 747 reconstruction.	333
Figure 8.29	Photograph showing the displacement of the cargo floor and frames in the aft direction.	333
Figure 8.30	Air Lanka Tristar, Sri Lanka, 1986.	334
Figure 8.31	Partly reassembled fuselage of Convair 580, Skagerrak, 1989.	335
Figure 8.32	Aluminum flake showing craters and rolled edges.	336
Figure 8.33	Damage to part of engine nacelle.	338
Figure 8.34	Peppering on landing gear wheel door.	339
Figure 8.35	(a) Embedded fragment as found and (b) after sectioning.	340
Figure 8.36	Fragment embedded in de-icer can bellows after passing through 13 thicknesses of metal.	340
Figure 8.37	(a) Hole with rusted nodule in de-icer can, as found, and (b) after sectioning to show the steel fragment.	340
Figure 8.38	Alignment of perforations in inner and outer wing skins.	341
Figure 8.39	Typical impact crater on outer skin.	342
Figure 8.40	Lockerbie, 1988.	343
Figure 8.41	Cargo container extrusion showing pitting.	344
Figure 8.42	Explosively formed impact crater on luggage-container frame extrusion.	345
Figure 8.43	Polymeric material deposited within an explosively formed crater.	345
Figure 8.44	Microsection through one of the impact craters showing deposited material.	346
Figure 8.45	Elemental X-ray distribution maps illustrating the compositional differences between the deposited material and the substrate.	347

Figure 9.1	Variation of pressure with time for an idealized vented gas explosion.	358
Figure 9.2	Breaking pressure as a function of area for 5 mm thick glass panes.	361
Figure 9.3	Mean breaking pressure of glass panes as a function of glass thickness.	362
Figure 9.4	Mean distance of travel of fragments of glass as a function of the explosion overpressure.	363
Figure 9.5	Decay of pressure with time for a classic shock wave.	365
Figure 9.6	Side-on shock overpressure– V –scaled range.	368
Figure 9.7	U-tube manometer used to test pipes for leaks.	372
Figure 9.8	Structural damage caused by a bursting electrically heated hot water cylinder.	374
Figure 9.9	Electrically heated hot water cylinder that had burst.	374
Figure 9.10	Thermal damage to a decorative wall covering caused by deflagration of a natural gas/air mixture.	375
Figure 9.11	Thermal damage to a paper towel caused by deflagration of a natural gas/air mixture.	375
Figure 9.12	Scorching to the bottom panels of a frying range caused by deflagration of a gasoline/air mixture.	376
Figure 9.13	Fire damage due to ignition of gas leaking from a broken pipe.	377
Figure 9.14	Secondary fire initiated by the deflagration of a gas/air mixture.	377
Figure 9.15	Chairs overturned by the upward displacement of the floor.	379
Figure 9.16	Plan of the basement and ground floor of the destroyed building.	382
Figure 9.17	The scene of the explosion.	383
Figure 9.18	Butane cylinder and gas ring recovered from basement.	384
Figure 9.19	Partially melted shrink wrap.	384
Figure 9.20	Reconstruction of the basement stairs.	385
Figure 9.21	Scorched splinters on the underside of the staircase treads and risers.	385
Figure 9.22	Routings of the gas main and service pipes.	385
Figure 9.23	Reconstruction of the new service pipe manifold and three gas meters.	386
Figure 9.24	Street plan of area of explosion; the explosion occurred in dwelling B.	388

Figure 9.25	Ground floor plan of dwelling B.	389
Figure 9.26	Rear view of the damaged building (dwelling B).	390
Figure 9.27	View of lounge showing scorched wallpaper, coffee table, and carpet, and the Baxi boiler.	390
Figure 9.28	The failed compression fitting.	391
Figure 9.29	Basic 9 mm sleeved pipe emerging from the external wall of the kitchen.	391
Figure 9.30	Close-up view of the defective compression joint.	391
Figure 9.31	Variation with time of gas concentration.	393
Figure 9.32	Plan of the ground floor of the building.	394
Figure 9.33	Fire on the ground floor in the area of the workshop, but no sign of fire in the area of the office.	396
Figure 9.34	Fire on the ground floor in the area of the workshop and in the area of the office.	396
Figure 9.35	The west elevation of the building, showing windows from the workshop in the foreground.	397
Figure 9.36	There was no evidence of smoke deposits on the remains of glazing in the workshop windows.	397
Figure 9.37	The external wall of the north elevation was structurally sound.	397
Figure 9.38	There were large cracks in the external brick wall of the south elevation and the brick panels were bowed slightly outward.	398
Figure 9.39	Scaffolding being erected to support the structure and provide a cage within which to work safely in the building.	398
Figure 9.40	Pool-shaped burn patterns in the carpet and underlay of the corridor on the east side of office 1, and localized fire damage to an office chair standing above one of the areas of floor damage.	399
Figure 9.41	Protection patterns on the floor of the darkroom where cardboard cartons had been standing during the fire, one of which possessed an odor of a hydrocarbon fuel.	399
Figure 9.42	Pool-shaped burn patterns in the floor at the south end of the workshop, where there were also patches of burnt carpet underlay.	400
Figure 9.43	Pool-shaped burn patterns extending from the south to the north ends of the workshop floor, where there were also patches of burnt carpet underlay.	400
Figure 10.1	The KENBOM post-blast scene (aerial perspective).	413

Figure 10.2	The KENBOM post-blast scene, lower roof level perspective; the point of detonation was approximately where the front-end loader is located in the center of the image.	414
Figure 11.1	Country of origin stamp and UPC sticker on a pipe.	433
Figure 11.2	Damage to a pipe caused by a low explosive (black powder).	433
Figure 11.3	Damage to a pipe caused by a high explosive (RDX: military C-4).	433
Figure 11.4	45-degree fractures produced by detonator initiation of double base smokeless powder.	434
Figure 11.5	Tool marks imparted by a vise to a pipe.	435
Figure 11.6	Post-blast remains of a dry cell battery.	438
Figure 11.7	Fingerprint on the adhesive side of a tape.	440
Figure 11.8	General analytical scheme for unreacted low explosives.	441
Figure 11.9	General analytical scheme for residues from low explosives.	449
Figure 11.10	Grains of black powder.	451
Figure 11.11	IR spectrum of black powder (potassium nitrate and sulfur).	451
Figure 11.12	Ion chromatogram of burned commercial black powder residue on a suppressed system.	453
Figure 11.13	Ion chromatogram of burned commercial black powder residue on an unsuppressed system.	454
Figure 11.14	Pyrodex grains.	455
Figure 11.15	IR spectrum of Pyrodex.	457
Figure 11.16	IC/MS chromatogram of burned Pyrodex using a suppressed system.	458
Figure 11.17	IC/MS chromatogram of post-blast Pyrodex residue using a suppressed system conditions.	458
Figure 11.18	Mass spectrum of the perchlorate ion.	459
Figure 11.19	Mass spectrum of the thiocyanate ion.	459
Figure 11.20	IR spectrum of sodium benzoate.	460
Figure 11.21	IR spectrum of sodium 3-nitrobenzoate.	461
Figure 11.22	IR spectrum of dicyanodiamide.	461
Figure 11.23	IR spectrum of Jim Shockey's Gold Powder.	462
Figure 11.24	Structural formula of ascorbic acid.	462
Figure 11.25	Common smokeless powder morphologies.	465
Figure 11.26	A mixture of smokeless powders.	466

Figure 11.27	GC/MS of smokeless powder additives.	468
Figure 11.28	HPLC of smokeless powder additives.	469
Figure 11.29	HPLC of smokeless powders from different batches.	470
Figure 11.30	Ion chromatogram of burned flash powder.	473
Figure 11.31	HPLC of a standard mix of sugars.	475
Figure 11.32	Material recovered from a pipe bomb in a suitcase.	481
Figure 12.1	Common oxidizers that can be made to produce IEs.	497
Figure 12.2	Common fuels mixed with oxidizers to produce IEs.	498
Figure 12.3	Well-labeled chemical precursors for IE production.	499
Figure 12.4	Less obvious chemical precursors for IE production.	499
Figure 12.5	AN prills.	501
Figure 12.6	Air-blast overpressure TNT equivalency of UNi over scaled distance.	505
Figure 12.7	Typical packaging for chlorates and perchlorates sold for pyrotechnic usage.	507
Figure 12.8	ESD sensitivity of potassium chlorate mixed with aluminum powder.	510
Figure 12.9	Ionization energy of the elements for lower groups.	511
Figure 12.10	Detonation velocity of TATP as a function of density.	516
Figure 12.11	Effect of aging of TATP friction sensitivity.	518
Figure 12.12	Relative GC/MS peaks of TATP residue with various storage media.	519
Figure 12.13	Detonation velocity of HMTD as a function of density.	521
Figure 12.14	Sample size needed for the TST.	524
Figure 12.15	FBI explosive chemistry examination flowchart.	529
Figure 12.16	Raman and IR spectra of ETN.	531
Figure 12.17	Raman and IR spectra of CTMTNA, R-salt.	532
Figure 12.18	IR Spectrum of hexamine.	533
Figure 12.19	IR spectrum of citric acid.	533
Figure 12.20	IR spectrum of urea.	534
Figure 13.1	Structure of TATP.	541
Figure 13.2	Structure of HMTD.	541
Figure 13.3	Sampling kit.	549

Figure 13.4	Vacuum sampling equipment for explosives trace recovery.	550
Figure 13.5	Extraction scheme for conventional organics, inorganics, and peroxides.	551
Figure 13.6	Solid phase extraction equipment.	552
Figure 13.7	TLC plate of standard explosives in toluene/ethyl acetate.	555
Figure 13.8	GC/TEA chromatogram of standard explosives.	558
Figure 13.9	GC/TEA calculation spreadsheet for a routine quality assurance analysis of a standard RDX solution.	561
Figure 13.10	Schematic diagram of APCI.	562
Figure 13.11	Tentative structure for a base peak with m/z 89 in the LC/MS of TATP.	564
Figure 13.12	Schematic of LC/MS/MS.	565
Figure 13.13	HMTD SRM chromatogram of m/z 207 to 118.	566
Figure 13.14	Plan of FEL trace facility.	569
Figure 14.1	SPME/GC/ECD of 14 standard explosives.	589
Figure 14.2	Standard explosives mixture separated by GC with a chemiluminescence detector on (a) a clean capillary column and (b) on an unprotected capillary column contaminated by a post-blast extract.	592
Figure 14.3	The analysis of a mixture of explosives using two different GC columns (RTX-TNT and RTX-TNT2) with differing polarities.	593
Figure 14.4	An example of a fast GC analysis using a microbore column coupled to a pulsed discharge ECD.	594
Figure 14.5	GC/FID analysis of two oil samples extracted from different lots of Semtex H plastic bonded explosive.	596
Figure 14.6	HPLC of a mixture of explosives.	598
Figure 14.7	HPLC/UV analysis of TNBS derivatives.	600
Figure 14.8	Analysis of a Winchester double-base ball powder via HPLC with UV detection at 230 nm.	601
Figure 14.9	SEC of different NCs using a TEA detector.	604
Figure 14.10	Gradient elution of a 5 ppm standard containing ions and interferences of interest in low explosives residue analysis.	605
Figure 14.11	The analysis of a series of different pipe bombs analyzed by IC using nonsuppressed conductivity detection with an isocratic eluent.	606
Figure 14.12	Separation of 5 ppm cation standards on a Dionex SCS 1 column.	608
Figure 14.13	Analysis of a the combustion residue of Black Mag, a black powder substitute, by HPLC-ESI-QTOF-MS.	609

Figure 14.14	Capillary electropherogram of Pyrodex pipe bomb residue anions.	611
Figure 14.15	Separation of a standard containing monovalent cations present in explosives.	612
Figure 14.16	Dual opposite injection of an aqueous standard of mixed anions and cations present in explosives.	613
Figure 14.17	Standard solution containing constituents present in smokeless powders.	613
Figure 14.18	Separation of a series of nitrate esters using a microfluidic CE system.	614
Figure 15.1	EI mass spectrum of 2,4-dinitrotoluene.	625
Figure 15.2	TIC of a mixture of explosives obtained by GC/MS.	626
Figure 15.3	Mass chromatograms of some explosives obtained by LC/MS in the negative-mode ESI.	626
Figure 15.4	EI mass spectrum of TNT.	628
Figure 15.5	CI mass spectrum of TNT, using methane as reagent gas.	629
Figure 15.6	Spectra of PETN, RDX and TNT recorded in APCI (A-C) and ESI (D-F).	634
Figure 15.7	EI/MS at a scan range 40–400 of NG (a), PETN (c) and CI/MS (using methane as reagent gas) of NG (b), PETN (d).	636
Figure 15.8	ESI mass spectrum of a mixture of high explosives containing EGDN, NG, TNT, PETN, RDX, and HMX in 50% MeOH/50% aqueous mixture with 0.3 mM ammonium chloride, ammonium formate, and ammonium nitrate.	638
Figure 15.9	EI mass spectrum of RDX.	640
Figure 15.10	CIMS of RDX, using methane (A) and isobutane (B) as reagent gases.	641
Figure 15.11	EI mass spectrum of TATP.	647
Figure 15.12	Positive ion mass spectrum of 10 ng TATP deposited on paper using MeOH/water (70:30) doped with NaCl (10 mM) as spray solvent.	651
Figure 15.13	EI mass spectrum of pentafluorobenzyl thiocyanate, identified in an actual case involving black powder.	653
Figure 16.1	IR spectrum of TNT.	675
Figure 16.2	IR spectrum of pentaerythritol tetranitrate.	675
Figure 16.3	IR spectrum of ethylene glycol dinitrate.	676
Figure 16.4	IR spectrum of nitroglycerin.	676

Figure 16.5	IR spectrum of nitrocellulose.	677
Figure 16.6	IR spectrum of metriol trinitrate.	677
Figure 16.7	IR spectrum of RDX.	678
Figure 16.8	IR spectrum of HMX.	679
Figure 16.9	IR spectrum of diazodinitrophenol (DDNP).	679
Figure 16.10	IR spectrum of urea nitrate.	680
Figure 16.11	IR spectrum of TATP.	681
Figure 16.12	IR spectrum of HMTD.	681
Figure 16.13	IR spectrum of sodium nitrate.	683
Figure 16.14	IR spectrum of potassium nitrate.	683
Figure 16.15	IR spectrum of ammonium nitrate.	684
Figure 16.16	IR spectrum of sodium chlorate.	684
Figure 16.17	IR spectrum of potassium chlorate.	685
Figure 16.18	IR spectrum of potassium perchlorate.	685
Figure 16.19	IR spectrum of potassium sulphate.	686
Figure 16.20	IR spectrum of mercury fulminate.	686
Figure 17.1	The AFP's Shimadzu ion chromatograph being utilized in a hotel room.	702
Figure 17.2	Schematic diagram of the relative location of a mobile laboratory in relation to the scene, sample receipt area, and forward command post.	703
Figure 17.3	Ion chromatogram of typical residue from scene of the Australian Embassy bombing in Jakarta.	708
Figure 17.4	Examples of unknown suspected explosive chemicals.	710
Figure 17.5	FTIR and Raman spectra used to identify unknown suspected explosive chemicals shown in Figure 17.4.	711
Figure 18.1	Protocol for analysis of an unknown residue suspected to be a high explosive.	731
Figure 18.2	GC/TEA analysis of a standard mixture.	733
Figure 19.1	Extensive fragmentation and mutilating injuries on a person located close to the epicenter of an explosion.	744
Figure 19.2	Traumatic amputation of the torso of a suicide bomber.	744
Figure 19.3	Radiant heat injuries of the face with evidence of singeing of hair.	745

Figure 19.4	Thermal damage to the hand of a bomb handler with evidence of charring.	745
Figure 19.5	Multiple peppering injuries consisting of abrasions, small lacerations, and contusions.	746
Figure 19.6	Multiple shrapnel entry wounds of different sizes.	747
Figure 19.7	Multiple shrapnel entry wounds resembling bullet wounds.	747
Figure 19.8	Multiple shrapnel irregular entry wounds.	747
Figure 19.9	Localized irregular entry wound on the left eye of a victim of a hand grenade attack.	747
Figure 19.10	Blast lung injury with extensive pulmonary hemorrhage.	748
Figure 19.11	Localized amputation of both hands and mutilating injuries in the torso and face of a handler of a hand grenade.	752

Series Editor's Note

International Forensic Science Series

The modern forensic world is shrinking. Forensic colleagues are no longer just within a laboratory but across the world. E-mails come in from London, Ohio, and London, England. Forensic journal articles are read in Peoria, Illinois, and Pretoria, South Africa. Mass disasters bring forensic experts together from all over the world.

The modern forensic world is expanding. Forensic scientists travel around the world to attend international meetings. Students graduate from forensic science educational programs in record numbers. Forensic literature—articles, books, and reports—grows in size, complexity, and depth.

Forensic science is a unique mix of science, law, and management. It faces challenges like no other discipline. Legal decisions and new laws force forensic science to adapt methods, change protocols, and develop new sciences. The rigors of research and the vagaries of the nature of evidence create vexing problems with complex answers. Greater demand for forensic services pressures managers to do more with resources that are either inadequate or overwhelming. Forensic science is an exciting, multidisciplinary profession with a nearly unlimited set of challenges to be embraced. The profession is also global in scope—whether a forensic scientist works in Chicago or Shanghai, the same challenges are often encountered.

The International Forensic Science Series is intended to embrace those challenges through innovative books that provide reference, learning, and methods. If forensic science is to stand next to biology, chemistry, physics, geology, and the other natural sciences, its practitioners must be able to articulate the fundamental principles and theories of forensic science and not simply follow procedural steps in manuals. Each book broadens forensic knowledge while deepening our understanding of the application of that knowledge. It is an honor to be the editor of the Taylor & Francis International Forensic Science series of books. I hope you find the series useful and informative.

Max M. Houck, PhD

Director, Forensic Science Initiative, Research Office

*Director, Forensic Business Research and Development, College of Business and Economics
West Virginia University*

Preface

In common with the first edition of *Forensic Investigation of Explosions*, my objective in the second edition has been to provide pertinent, up-to-date and multidisciplinary information in one volume broadly covering explosives, explosions, detection of hidden explosives, processing scenes of explosion, case management, quality assurance, science, engineering, medicine and the law.

In the thirteen years since the first edition was published, significant advances in science and technology have been applied to detection of explosives, investigation of scenes of explosion and analysis of explosives and their residues. There has been on-going advancement in standards for quality assurance and training. This era has also seen increased world-wide use of improvised explosives and devices. The second edition addresses these and related issues both in updated content from the first edition and expanded content from new authors. New chapter topics are improvised explosives, vehicle-borne improvised explosive devices, casework management and portable explosive detection instruments. Courts of law remain the ultimate arbiters of what is acceptable forensic practice. Therefore, pertinent legislation underlying explosives case investigations is included in this edition.

The authors of this book are internationally recognized experts in their fields and it was a pleasure working with such talented people. I sincerely thank them for their time and dedication in sharing their expertise. I appreciate them producing their chapters in the face of the often grueling time demands of their professions. I also thank my commissioning editor, Becky Masterman, and my wife for their support and understanding as my own timelines stretched.

Alexander (Sandy) Beveridge
Vancouver

Contributors

Maurice Baker

Maurice Baker, a chartered engineer, retired in 1997 from the UK Defence Evaluation and Research Agency. His expertise includes failure analysis and studies of materials, pyrotechnics, and explosives, but his particular specialization is the study of the microeffects of explosions on materials. He has worked on 12 incidents of suspected aircraft sabotage. His corrosion expertise has been particularly relevant when aircraft have crashed into the ocean.

Curtis Bell

Dr. Curtis Bell is a physicist at the Transportation Security Laboratory, part of the Department of Homeland Security Science and Technology Directorate. Curtis received his PhD from Rutgers University and has expertise on detection of explosives using X-ray or nuclear detection technologies.

Edward C. Bender

Ed Bender is a forensic chemist in the explosives section of the Bureau of Alcohol, Tobacco, Firearms, and Explosives (ATF) in the U.S. Department of Justice. A past member of the ATF National and International Response teams, he serves as an instructor in the chemical analysis of explosives, post-blast investigations, and homemade explosives courses in various venues both nationally and internationally and has numerous publications in the field of forensic science over the past 30 years.

Sarah Benson

Dr. Sarah Benson is deputy coordinator of criminalistics and identification sciences in the Forensic and Data Centers portfolio of the Australian Federal Police. She manages both the Chemical Criminalistics and Document Sciences teams. During her career, Sarah has deployed to Indonesia and the Philippines to assist local authorities with the examination of post-blast scenes and the provision of subsequent laboratory support. She has developed guidelines for the examination of secondary scenes in relation to Australian explosive incidents and maintains a keen interest in research and development.

Pamela Beresford

Dr. Pamela Beresford is a technical editor with GST, Inc., working at the Transportation Security Laboratory (TSL), part of the Department of Homeland Security Science and Technology Directorate. Pamela received her PhD in biology from the City University of New York and focuses on biosensors as well as technical report production at the TSL.

Alexander D. Beveridge

Dr. Alexander (Sandy) Beveridge is the editor of the first and second editions of this book. He is a consultant forensic chemist and lawyer in Vancouver, Canada and has over 30 years of experience in explosives casework, research and training. He was formerly a forensic scientist in the Forensic Laboratory Service of the Royal Canadian Mounted Police.

Sharon Broome

Sharon Broome is a principal case officer in the Forensic Explosives Laboratory of the UK Defence Science and Technology Laboratory. She is a chartered chemist and a fellow of the Royal Society of Chemistry with 18 years of experience in examining over 150 forensic cases, many involving improvised explosive devices, their component parts, and post-explosion scenes. Notable cases include a number of IRA incidents, the UK response to the Bali bombings, the July 2005 London bombings, the car bomb attack at Glasgow airport in 2007, and the examination of debris from incidents arising from military operations.

Inge Corbin

Inge Corbin is a doctoral student at Florida International University in Miami studying trace detection of improvised explosives. She also is a forensic chemist at the Dade-Miami Police Department Crime Laboratory and a fellow of the American Board of Criminalistics.

Sean Doyle

Sean Doyle is a chartered chemist and a fellow of the Royal Society of Chemistry. He has over 30 years experience as a forensic scientist, the last 20 in the field of explosives investigation. In addition to casework, Sean has had significant international involvement in research, education, and the development of quality systems as they apply to the practice and delivery of forensic science. Sean was, until March 2010, the principal scientist at the Forensic Explosives Laboratory, Defence Science and Technology Laboratory, Fort Halstead, England, having previously been head of forensic chemistry and research. He is now a director of Linked Forensic Consultants Ltd (<http://www.linkedforensics.com>).

Christopher D. Foster

Dr. Chris Foster joined Dr. J. H. Burgoyne & Partners, consulting engineers and scientists in London, UK, in 1972. He subsequently became managing partner and is well known internationally for his work in conducting investigations into the causes of explosions and fires in buildings and ships. Chris is a regular contributor to technical courses on fire science and fire investigation.

John H. Garstang

John Garstang is a mechanical engineer and commercial pilot. He retired from the Transportation Safety Board of Canada after 32 years service, where he was a member of the national response team, mandated to investigate air, marine, rail, and commodity pipeline accidents and incidents. His expertise includes failure analyses and the study of fire and explosions. He does contractual work for agencies such as Defence Research and Development Canada, and he serves as an instructor at the Canadian Police College.

Polly Gongwer

Dr. Polly Gongwer is a trace chemist at the Transportation Security Laboratory, part of the Department of Homeland Security Science and Technology Directorate. Polly received a PhD in chemistry from the University of Delaware and has devoted her postgraduate career to biological and technological detection of explosives.

Susan Hallowell

Dr. Susan Hallowell is the director of the Transportation Security Laboratory, part of the U.S. Department of Homeland Security Science and Technology Directorate. Susan began her career as a research chemist for the U.S. Army, in the area of detection of and protection against chemical warfare agents, and after earning a PhD in analytical chemistry (sensor development) from the University of Delaware, shifted to explosives detection for aviation security. Susan is a senior executive fellow from the John F. Kennedy School of Government at Harvard University.

Steve Harris

Steve Harris is a chartered engineer and a member of the Institution of Mechanical Engineers and the Royal Aeronautical Society. He is the leader of the Forensic Engineering and Corrosion Control group at QinetiQ in Farnborough, UK, and has contributed to numerous accident investigations. He previously managed a research program into the vulnerability of civil aircraft to explosions.

Nigel Harrison

Nigel Harrison is a technical leader within the Forensic Engineering Team at QinetiQ in Farnborough, UK, specializing in metallurgical failure analysis and materials characterization. He has contributed to many investigations and accident enquiries, including a number of explosive-related incidents.

Robert B. Hople

Bob Hople retired in 1996 from his position as corporate manager of technical services with Dyno Nobel, Inc., in Salt Lake City, Utah, after 35 years in the explosives industry and 4 years in the mining industry. He holds a master's degree in mining engineering from the Missouri School of Mines. He enjoys historical research in the explosives field.

James W. Jardine

Judge Jim Jardine is a senior judge in the Provincial Court of British Columbia, Canada. As a lawyer, he received the professional honor of Queen's Counsel in 1984. His experience as a prosecutor included several high-profile terrorist cases involving explosives. He was formerly in private practice in Vancouver, where he acted for both prosecution and defense.

Indira Kitulwatte

Dr. Indira Kitulwatte is a forensic pathologist and a senior lecturer in forensic medicine at the University of Kelaniya, Sri Lanka. She holds graduate and post-graduate degrees from the University of Colombo and served a 2-year clinical fellowship in forensic pathology at

the Forensic Pathology Service of Ontario, Canada. She is active in research and has made many presentations to national and international conferences.

Ronald Krauss

Dr. Ronald Krauss is the bulk technology lead at the Transportation Security Laboratory, part of the Department of Homeland Security Science and Technology Directorate. Ronald received a PhD in experimental physics from Texas A&M University and has expertise in detection of explosives using X-ray, neutron, gamma ray, and electromagnetic interrogation technologies.

Richard Lareau

Dr. Richard Lareau is the chief scientist at the Transportation Security Laboratory, part of the Department of Homeland Security Science and Technology Directorate. Richard earned a PhD in analytical chemistry from Arizona State University and is an expert in mass spectrometry, electronic materials, and nanotechnology.

Bruce R. McCord

Dr. Bruce McCord is a professor of analytical and forensic chemistry at Florida International University. He joined the faculty in 2004 from Ohio University, where he was director of the forensic chemistry program. Previously, Bruce was a researcher in the FBI Forensic Science Research and Training Center in Quantico, Virginia. His research interests involve development of liquid-based separation methods in chromatography and their forensic applications, including explosives residue detection.

Bibhu Mohanty

Dr. Bibhu Mohanty is a professor emeritus in the Department of Civil Engineering at the University of Toronto, Canada. Previously he held the NSERC chair in rock dynamics and fragmentation at the same institution. Prior to that, he headed the blasting physics research group at ICI Explosives Americas and also taught at McGill University, Montreal. His research interests are in the areas of detonation physics, explosion hazards, and rock blasting.

Gerard T. Murray

Dr. Gerry Murray retired from Forensic Science Northern Ireland (FSNI) in August 2007 as principal scientific officer following 34 years of service in the Explosives Section. Subsequently, he has provided a forensic explosives investigation consultancy service to FSNI. His experience has covered all aspects of the terrorist use of explosives in Northern Ireland. He has testified in many explosives-related cases and served on several Commissions of Inquiry. In 1994, Dr. Murray was appointed an officer of the Order of the British Empire (OBE) for his service.

Vincent Otieno-Alego

Dr. Vincent Otieno-Alego has worked for over 20 years as a chemical analyst in a number of research institutions and in government. He is a senior scientific officer with the Australian Federal Police and is serving as an adjunct associate professor at the University of Canberra. His expertise includes the use of an expansive range of laboratory and field-based analytical techniques for examining trace evidence for criminalistic purposes.

Michael S. Pollanen

Dr. Michael Pollanen is the chief forensic pathologist for the Ontario Forensic Pathology Services in Canada, and director of the Centre of Forensic Science and Medicine at the University of Toronto. He has published widely on topics in forensic pathology and is a consultant in forensic pathology to national and international organizations including the United Nations, Canadian International Development Agency, the International Criminal Court, and nongovernmental human rights organizations. He and the other pathologists in the Ontario Forensic Pathology Services perform medicolegal autopsies on Canadian soldiers who die during overseas deployments.

Joshua Rubinstein

Dr. Joshua Rubinstein is the human factors technology lead at the Transportation Security Laboratory, part of the U.S. Department of Homeland Security Science and Technology Directorate. Josh received his PhD in cognitive psychology from the University of Michigan and is focused on optimizing the user's experience with the broad array of explosives detection technologies.

Donald J. Sachtleben

Don Sachtleben retired from the Federal Bureau of Investigation in 2008 after 24 years of service specializing in counterterrorism and bombing investigations. He was supervisory special agent at the FBI Laboratory Explosives Unit and worked as a team leader on many major cases involving bombings in the United States and on U.S. interests outside the country. He founded Raptor Consulting LLC, which provides training and security consultation services.

Naomi Speers

Dr. Naomi Speers is team leader of chemical criminalistics within the Forensic and Data Centers portfolio of the Australian Federal Police. Since joining the AFP in 2002, Naomi has been involved in post-blast examinations in Indonesia and major proactive counterterrorism investigations in Australia.

Richard A. Strobel

Rick Strobel has been the chief of the explosives section of the U.S. Bureau of Alcohol, Tobacco, Firearms, and Explosives (ATF) since 1989. His areas of expertise include forensic explosives casework and training, arson analysis, and canine detection of accelerants and explosives.

Tsippy Tamiri

Dr. Tsippy Tamiri is a PhD graduate of Technion, Israel Institute of Technology, in Haifa. Since 1978, she has served as a forensic scientist in the Division of Identification and Forensic Science (DIFS) of the Israeli Police, specializing in the identification of drugs, explosives, and poisons, mainly by mass spectrometry. Her main research interests lie in the development of analytical methods for post-blast analysis. Tsippy has written a chapter on explosives analysis in the *Encyclopedia of Forensic Science* and published many papers, mainly in the field of explosives analysis.

Clifford Todd

Cliff Todd is principal forensic investigator with overall responsibility for forensic casework operations in the Forensic Explosives Laboratory at the UK Defence Science and Technology Laboratory. During his 22 years of service, Cliff has conducted in excess of 200 forensic explosives casework investigations, many involving improvised explosive devices, their component parts, and post-explosion scenes. He has given evidence in many cases including the July 7 and July 21 London bombings with respect to the overall design, functioning, intention, and potential effects of the various devices. In 2009 he was appointed an officer of the Order of the British Empire (OBE) for his service.

Jean-Yves Vermette

Jean-Yves Vermette has been the post-blast consultant for the Explosives Disposal and Technology section of the Royal Canadian Mounted Police since 1989. His activities include training, conducting test explosions, and post-blast investigations in and outside Canada.

James C. Weatherall

Dr. Jim Weatherall is a physicist with SRA, Inc., working at the Transportation Security Laboratory, part of the Department of Homeland Security Science and Technology Directorate. Jim conducts research in the direct physical measurement of energetic materials and in other personnel screening technology areas. His degrees are from Caltech and the University of Colorado, where he received his PhD in plasma physics. He holds patents for microwave sources and hazardous-liquid screening.

John Winn

John Winn was head of metal physics at the UK Defence Evaluation and Research Agency (DERA) from 1986 until his retirement in 1995. His interests included the development and application of X-ray and electron optical techniques to a wide variety of materials. He was a front-line investigator at many air crash incidents worldwide (including Lockerbie) with responsibility for their subsequent examination at DERA.

Kirk Yeager

Dr. Kirk Yeager is a senior forensic scientist with the U.S. Federal Bureau of Investigation (FBI) Laboratory. He is also a senior adjunct research scientist at New Mexico Tech. He has a PhD from Cornell University and has been synthesizing and studying energetic materials since 1993. He specializes in the study of improvised explosives and has served as a post-blast investigator with the FBI since 2000.

Shmuel Zitrin

Dr. Shmuel Zitrin is a PhD graduate of the Weizmann Institute of Science, Rehovot, Israel. During 1970–2000, he served as a forensic scientist in the Division of Identification and Forensic Science of the Israeli Police, working mainly in mass spectrometry and the analysis of explosives. His group was the first to identify triacetone triperoxide in a terror-related case. Shmuel is coauthor (with J. Yinon) of two books on the analysis of explosives. He has written chapters in several books and published many papers. Since his retirement in 2000, he has been teaching forensic science in academic institutions.

Editor

Alexander Beveridge

Dr. Alexander (Sandy) Beveridge is a consultant forensic chemist and lawyer in Vancouver, Canada. He is editor of the first and second editions of this book. A fellow of the Chemical Institute of Canada and a PhD graduate of the University of Glasgow, he was a forensic scientist in the Royal Canadian Mounted Police (RCMP) Forensic Science Service for over 30 years, laterally as head of the chemistry section of the Vancouver laboratory. Throughout his career he has undertaken numerous explosives cases, including international involvement and investigative task force membership. He has been actively involved in research and training in the explosives' residue and trace chemical evidence fields and has testified, published and lectured widely on these topics. He has served on three explosives-related committees of the U.S. National Research Council.

Following retirement from the RCMP in 1998, Sandy became a practicing lawyer, which has provided a fresh perspective on forensic science. Concurrently, as an independent forensic scientist, he combines his scientific and legal knowledge to provide consulting and teaching services to investigators, scientists, lawyers and students at academic institutions.

The History, Development, and Characteristics of Explosives and Propellants

1

ROBERT B. HOPLER

Contents

1.1	Introduction	1
1.2	Propellants	2
1.2.1	Black Powder	2
1.2.2	Smokeless Powder	3
1.3	Military Explosives	4
1.3.1	Picric Acid	4
1.3.2	Trinitrotoluene	5
1.3.3	Tetryl	5
1.3.4	Pentaerythritol Tetranitrate	5
1.3.5	Research Department Explosive and High Melting Explosive	6
1.3.6	Plastic Explosives	6
1.3.7	General Overview	7
1.4	Commercial Explosives	7
1.4.1	Nitroglycerin	8
1.4.2	Dynamite	8
1.4.3	Liquid Oxygen Explosives	10
1.4.4	Ammonium Nitrate	10
1.4.5	Ammonium Nitrate/Fuel Oil	11
1.4.6	Slurry Explosives	12
1.4.7	Emulsion Explosives	12
1.5	Improvised or “Do-It-Yourself” Explosives	15
1.6	Methods of Explosives Initiation	16
1.7	Summary	17
	References	17

1.1 Introduction

The history of explosives and propellants, also known generally as “energetic materials,” begins with the material known as gunpowder or black powder, whether the intended use was for civil applications such as rock blasting, military uses in demolition, shell filling (bursting charges) and construction projects, or military and civilian propellant charges for shotguns, pistols, rifles, or artillery. The individual inventor of black powder will undoubtedly forever remain unknown, but numerous writers, such as Drinker (1878), Munroe (1888), Marshall (1915), and Davis (1941, 1943), have described what is known about its

development and evolution; therefore, there will be no such discussion here. Suffice to say that until the discovery of nitrated explosive compounds such as nitrocellulose by Schönbein and Böttger (independently of one another) and nitroglycerin by Sobrero (all occurring in 1846), the only explosive available for *any* purpose was black powder.

For purposes of this discussion, the subject will be divided into three categories:

- Solid (particulate) propellants
- Military explosives
- Commercial explosives

Explosives are further classified into high and low explosives, which are differentiated on the basis of their means of propagation of the explosive reaction through the material. High explosive reactions progress by a shock wave, and their velocity is defined as progressing at higher than the speed of sound in the undetonated material. Low explosive reactions progress by grain burning, and the reaction speed is at less than the speed of sound in the explosive medium. Other classifications designated by government agencies for storage, transportation, or other activities, such as “high explosive” and “blasting agent,” which have to do with the magnitude of the impetus necessary for their initiation, do not change the fact that they are both high explosives.

Also, in the attempt not to make this discussion overly broad, this chapter stresses U.S. practices, explosive history, and developments.

1.2 Propellants

Propellants may be granular, solid, or liquid. The primary focus is on granular (particulate) material since they are the most commonly encountered by the forensic chemist. A solid propellant is a deflagrating material designed to accelerate a projectile from its position of rest at the breech of a weapon to its full velocity as it exits the tube or barrel.

In the ideal (and designed-for) case the complete consumption of the propellant and the exit of the projectile will occur at the same instant. Propellant grains are thus chemically formulated and physically designed to achieve this end. The grains burn particle-to-particle at speeds below the speed of sound in the material: this defines the word “deflagrating.” Historically, such materials have been called “progressive” powders. In addition to burning particle-to-particle, each particle burns from its free surface inward, or, in the case of perforated grains, also from the free surface outward. This characteristic enables the propellant designer to size and configure the grains or particles to be totally consumed at the optimum instant. Propellant grains may be found in a multitude of shapes and sizes, as might be expected given the varieties of weapons and desired pressures and projectile velocities.

1.2.1 Black Powder

Black powder is a mixture of three components, generally (and originally) charcoal, sulfur, and potassium nitrate. These are typically in the mass ratio of 15:10:75. Many variations to that ratio have been used; Cundill (1889) lists over 20 varieties, many with sub-varieties. Most of the differences, however, are insignificant. The one major development in the past 100 years is the use of sodium nitrate in some black powder grades.

Black powder has an inherent drawback as a military propellant due to the fact that it produces a solid reaction product. Because of this, a dense black cloud is produced upon firing a weapon. This has two adverse results: the position of a firing weapon is readily apparent, and after a number of rounds are fired the volume of battlefield smoke leads to confusion and general chaos. For this reason the development of a “smokeless” propellant charge was the objective of every government’s weapons laboratory. Upon the discovery of the nitration reaction, this research intensified.

1.2.2 Smokeless Powder

The early history of the nitrated carbohydrates, which includes the 1833 discovery of nitro-starch (called *xyloidine* by its discoverer, Braconnot) and guncotton, called *pyroxyline* or *pyroxyle* by the chemist Pelouze, is thoroughly covered by Davis (1941, 1943).

Guncotton, nitrocellulose of high nitrogen content (13.35%–13.45%), was the first nitrated material to be tried as a replacement for black powder, but it was too prone to accidents. However, its military use continued after it was found that the newly invented mercury fulminate blasting cap would cause compressed guncotton to detonate, leading to its application as a demolition charge and shell filling. Its use was rather short-lived, however, due to the introduction of picric acid.

Research continued on nitrocellulose of lower nitrogen content as a propellant material, and the first good smokeless rifle powder was produced by Vieille in 1886, for the French government. This was nitrocellulose with ether alcohol, kneaded in a bread-making type machine, rolled out into thin sheets, and then cut into small squares and dried (Military Explosives 1924). This was a “single-base” smokeless powder (nitrocellulose only).

In 1888, Nobel invented a powder he called *ballistite*, which was a low-nitrated nitro-cotton gelatinized with nitroglycerin; this became known as “double-base” powder. In the same year *cordite* (given that name because it was extruded in the form of a cord or ribbon), a mixture of high-nitrated guncotton, nitroglycerin, and Vaseline, gelatinized by means of acetone, was developed by an English committee (Marshall 1915).

Later, “triple-base” smokeless powders were developed, containing nitroguanidine in addition to the nitro-cotton and nitroglycerin of typical double-base powders. Triple-base powders were cooler-burning than the single- or double-base materials and use was mainly restricted to large-caliber weapons.

Developments in smokeless powder since those early days have been primarily to improve stability, decrease the erosion of the barrel of the weapon, control pressures, decrease smoke output (“smokeless” powders are smokeless in comparison to black powder, but still produce visible smoke), and decrease the muzzle flash from a firing weapon. The geometry of powders may include flakes, tubes, cylinders, sticks, flattened balls, or spheres (see Chapter 11, Figures 11.20 and 11.21).

The reader desiring a detailed background in the field of smokeless powders and other propellant materials should refer to the 10-volume *Encyclopedia of Explosives and Related Items* (referred to below as *Encyclopedia*), and to the publication *Propellant Profiles* (Wolfe 1991).

Table 1.1 illustrates typical formulations of the three general classes of smokeless powders. Some formulations may contain dye ingredients for the identification of particular brands, especially in commercial products.

Table 1.1 Smokeless Powder Composition

	M6	M5	M15	Function ^b
Nitrocellulose (13.15% N)	87		20.00	e
Nitrocellulose (13.25% N)		81.95		e
Nitroguanidine			54.70	c, e
Nitroglycerin		15.00	19.00	e
Potassium nitrate		2.15		f
Ethyl centralite		0.60	6.00	d, g, k
Graphite		0.30		a, h
Diphenylamine	1 ^a			k
Dinitrotoluene	10			e, g, i, j
Dibutyl phthalate	3			f, h
Sodium aluminum fluoride			0.30	b
Total	100	100.00	100.00	

Sources: *Encyclopedia of Explosives and Related Items, 1960–1975*. Vol. 1–7. Dover, NJ: Picatinny Arsenal. *Encyclopedia of Explosives and Related Items, 1978–1983*. Vol. 8–10. Dover, NJ: U.S. Army Research and Development Command. With permission.

^a Added to mix.

^b a, antistatic; b, cooling rate modifier; c, coolant; d, deterrent; e, energizer; f, flash suppressant; g, gelatinizer; h, hygroscopicity reducer, i, inhibitor; j, plasticizer; k, stabilizer.

1.3 Military Explosives

Just as black powder was the first propellant, so too was it the first military explosive. It was used for shell fillings, demolition, and military construction projects from the earliest times up until the invention of nitroglycerin.

Military explosives as discussed here are those used as the shell filling or “bursting charge” in artillery rounds and those used for demolition charges. Military construction projects typically use commercial-type explosives, except in field-expedient situations. The brief use of guncotton as a military explosive was noted above.

1.3.1 Picric Acid

By the early 1900s picric acid (2,4,6-trinitrophenol) had become the shell filling of choice of most of the world’s military forces. The Russians were the first to work out methods of production and use it as a shell filling, in 1894 (*Encyclopedia*, Vol. 8, 286). Picric acid went under many names; *lyddit* in England; *mélinite* in France; *sprengkorper* in Germany; and *shimoza* in Japan, to name but a few. Other picrates, especially ammonium picrate (“Explosive D,” $C_6H_2(NO_2)_3 \cdot NH_4$), have been widely used in fillings for armor-piercing shells, due to their extreme insensitivity to shock. In World War I this material was used in large-caliber shells. In World War II a mixture of ammonium picrate and trinitrotoluene (TNT) was widely used in the press-loading of armor-piercing shells.

Picric acid is part of the most important family of military explosives, all based on trinitrobenzene. The structural formulae of picric acid and some of its derivatives are shown in Figure 1.1 from Cooper and Kurowski (1996). This figure is one of the best illustrations of the relationship of these aromatic nitrate explosives to one another.

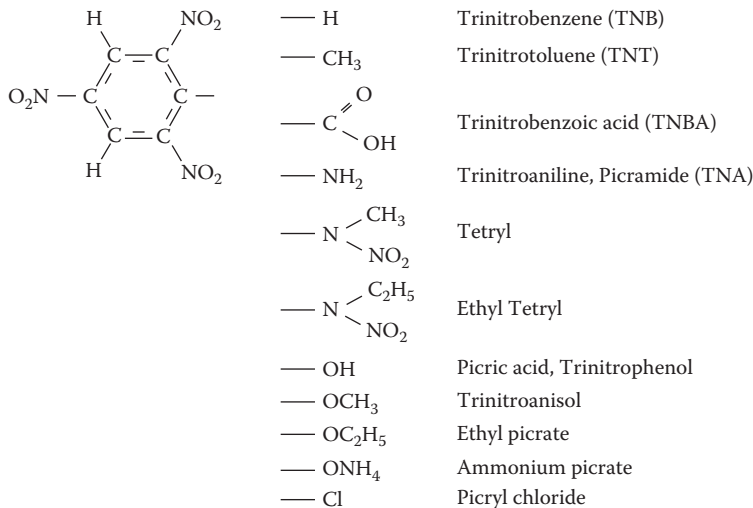


Figure 1.1 A family of explosives based on various monosubstitutions of a single hydrogen in 1,3,5 trinitrobenzene. (From Cooper, P. W. and S. R. Kurowski. *Introduction to the Technology of Explosives*, New York: Wiley-VCH Publishers, Inc., 1996. With permission.)

1.3.2 Trinitrotoluene

During and after World War I the explosive trinitrotoluene (TNT; $C_7H_5N_3O_6$) became the dominant shell-filling and demolition-charge material. TNT has the advantage of being very easy to cast, since it has a wide spread between its melting and decomposition temperatures. One disadvantage is its extreme insensitivity in the cast form; where necessary, this is overcome in practice by adding a core of tetryl ($C_7H_5N_5O_8$). In order to conserve TNT for small caliber shells in World War I, a mixture of TNT and ammonium nitrate (“amatol”) was developed. It was specified for use only in shells of 4.7-inch to 9.2-inch diameter (Crowell 1919) but in actual practice it was used in all sizes.

For the same reason of conserving TNT, nitrostarch explosives were used very successfully in that war for hand grenades and trench mortar shells (Williams 1920). The structural formula of TNT is shown in Figure 1.2.

1.3.3 Tetryl

Tetryl (2,4,6-trinitrophenylmethyl nitramine, *N*-2,4,6-tetra-nitro-*N*-methyl aniline, or picryl-methyl nitramine) (see Figure 1.1) was used in military boosters, but has generally been replaced by materials such as research development explosive (RDX) and high melting explosive (HMX).

The *tetrytols* are mixtures of tetryl and TNT, which were utilized in boosters, demolition charges, shells, and shaped charges. The TNT generally made up 20%–35% of the mixture. An advantage of tetrytol is that it allows the casting of the explosive into munitions rather than requiring pressing. It is also more powerful than TNT, but not as sensitive as tetryl alone (*Encyclopedia*, Vol. 9, T165).

1.3.4 Pentaerythritol Tetranitrate

PETN (pentaerythritol tetranitrate, $C(CH_2ONO_2)_4$), first prepared in 1891, became commercially available in the 1930s in detonating cord and blasting caps. It is a component in

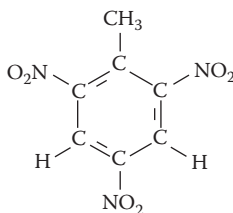


Figure 1.2 Structural formula of TNT.

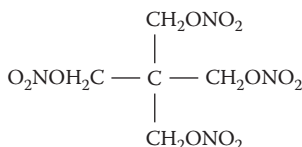


Figure 1.3 Structural formula of PETN.

many military explosives, most notably pentolite, where it may comprise 10%–60% of a mixture with TNT. Figure 1.3 shows the structural formula of this nitrate ester explosive.

1.3.5 Research Department Explosive and High Melting Explosive

Between the World Wars a number of explosives were developed, and after the start of the second war a vast amount of explosives research took place. One of the most important and useful military explosives is RDX, which was discovered in 1899 but not used until World War II. It is also called cyclonite, hexagen, and cyclo-trimethylenetrinitramine. HMX is another explosive used for military applications during and after World War II. The initials are said to stand for “high melting explosive,” although other sources for the acronym are sometimes cited. It is also called cyclo-tetramethylenetetranitramine or octogen. Figures 1.4 and 1.5 show the structural formulae for these nitramine explosives.

A vast number of explosives consisting of mixtures of various explosive compounds were developed by the combatants in World War II. Many of these combinations may include materials such as HMX, RDX, TNT, aluminum powder, wax, and plasticizers, with or without other ingredients for special properties. A few worth mentioning are Composition B (60% RDX/40% TNT/plus wax), Cyclotol (60%–75% RDX/25%–40% TNT), Torpex 2 (42% RDX/40% TNT/18% Al), and Composition C-4 (91% RDX/9% plasticizer).

1.3.6 Plastic Explosives

Plastic-bonded explosive, or PBX, explosives are a fairly recent development in the military arena. They are characterized by high mechanical strength, high detonation velocity, excellent stability, and insensitivity to shock and high temperatures. They cover a wide range of formulations, usually containing some ingredients from the list of RDX; PETN; HMX; aluminum; binders such as nylon, polyurethane, rubber, or similar material; and a plasticizer. Two of the best known are C-4 (see above) and SEMTEX (RDX/PETN), an explosive manufactured in the Czech Republic, which has been widely used in terrorist bombings.

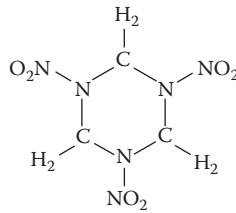


Figure 1.4 Structural formula of RDX.

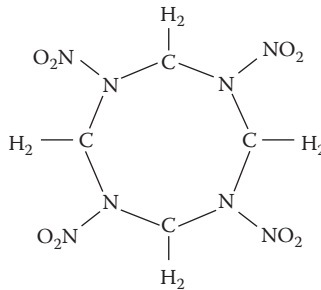


Figure 1.5 Structural formula of HMX.

1.3.7 General Overview

It is apparent that a great number of varieties of military explosives are available, each having unique features of detonation velocity, stability, brisance, and resistance to initiation by rifle bullet impact or shock. Some specialized explosives developed by the nuclear research laboratories even have the ability to withstand extremely high temperatures, such as those experienced upon reentry into the atmosphere by a ballistic missile.

Due to this great range of materials, this section is necessarily only a very brief overview of the field. The reader is referred to the references cited for further information. The *Encyclopedia* volumes from 1960 to 1983 and Williams (1920), both published by the U.S. Army, should be referred to for details of military explosive materials. For general explosives chemistry, the 4-volume series by Urbanski (1964) is an excellent reference.

Table 1.2 shows the density and detonation velocity for some of the explosives mentioned above. These are all from one reference (Research and Development of Materiel 1963) but sources frequently will disagree on some of these characteristics due to physical form (e.g., grain size) or test methods. Thus, this table should only be used for a general idea of characteristics.

1.4 Commercial Explosives

As noted above, military explosives, propellants, and commercial explosives all have the same ancestor: black powder. It is interesting to note that although black powder was noted as being used in warfare in very early times, its use in mining was not recorded until 1627. After that date there is a multitude of references to its use, but not before. The reason is probably that for its use in mining, someone had to devise a way to initiate the powder after the person was out of the area. In using the powder in a cannon, the gunner stands

Table 1.2 Military Explosives: Density and Velocity

Explosive	Density (g/cm ³)	Velocity (m/s, 1"φ)
Amatol (50/50)	1.55	6430
Composition C-4	1.59	8040
Composition B	1.68	7840
HMX	1.84	9124
Pentolite (50/50)	1.66	7465
PETN	1.70	8300
Picric acid		
(Pressed)	1.64	5270
(Cast)	1.71	7350
RDX	1.65	8180
Tetratol (20% TNT)	1.60	7385
Tetryl	1.71	7850
TNT	1.56	6825
Torpex	1.81	7495

Source: Data from *Research and Development of Materiel—Engineering Design Handbook*, Washington, DC: U.S. Army Materiel Command, 1963.

immediately beside the weapon in perfect safety—this is obviously not the situation with powder in a borehole! Once a “delay” type of material was developed (a powder-filled straw, for example), the breaking of rock became a great deal easier than it had been by hand or with fire-setting methods. A codevelopment was probably a metal drill sufficiently hard to bore a hole in the rock face for the powder.

1.4.1 Nitroglycerin

Alfred Nobel, noted previously for his invention of ballistite, took Sobrero’s discovery of nitroglycerin (glyceryl trinitrate) and made it a useful explosive by inventing the detonating blasting cap. This replacement for the spit from burning safety fuse was necessary because the *detonating* explosives need a shock wave for their reaction to start—the *deflagrating* explosives needed only a spark or flame (Hopler 1992).

The first use of nitroglycerin in mining was in the liquid form, with it either poured into downward-looking boreholes or encased in cans and slid into horizontal or “up” holes. In any case it was hazardous to ship and use. After tests with absorbent materials in an effort to make nitroglycerin easier to handle, Nobel settled upon diatomaceous earth (also known as kieselguhr or diatomite) in 1866. He named his mixture (at first 75% nitroglycerin/25% diatomaceous earth) *dynamite*. Figure 1.6 shows the structural formula for nitroglycerin, a nitrate ester.

1.4.2 Dynamite

Over the years, formulas for dynamite have been developed to fit every type of rock blasting. Varieties have been developed for severe water conditions, utilizing nitrocotton to gel the nitroglycerin (the “gelatins” are one branch of the dynamite family); for cohesiveness to enable loading into “up” holes in mines; for safe usage in underground coal mines (the

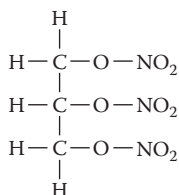


Figure 1.6 Structural formula of nitroglycerin.

“permissibles” having salts of various types to cool the explosive reaction as part of the formula) (Hopler 1996); and for economics by making formulas with very high ammonium nitrate percentages (and thus no cohesiveness or water resistance), where severe field conditions do not exist. Literally thousands of different formulas might be found, but for years all had the basic commonality of having nitroglycerin as a component.

For all of its good explosive characteristics, nitroglycerin has the very undesirable property of having a high freezing point, in the area of +50°F (+10°C). When dynamite is totally frozen it is relatively safe, unless one tries to break a cartridge. The danger (and the source of untold deaths in the first 50 years of dynamite) is when the miner tries to thaw the stick to use it in a borehole. Unless thawed slowly, with controlled temperatures, the material is very dangerous. Every explosives company catalog from the early days pictures “thawing kettles” or other recommended devices for the thawing procedure. Many approaches were taken to solving the problem. Nitrostarch was successfully introduced by DuPont as the main explosive ingredient (sensitizer) for “nonfreezing” dynamites, and that material later served as the basis for all the dynamite products of the Trojan Powder Company. However, problems of low sensitivity and lack of water resistance prevented nitrostarch dynamites from ever becoming more than a niche product. TNT and related compounds are also found in various companies’ “low freezing” or “arctic” dynamites.

In the mid-1920s, the automobile industry was experiencing fast growth, and an anti-freeze superior to alcohol was needed. Ethylene glycol was found to be excellent for this application. That liquid had also been known for years as an excellent nitroglycerin substitute when nitrated, and when co-nitrated with nitroglycerin (at a ratio of 60% ethylene glycol/40% glycerin) the mixture had a freezing point of about -40°F (-40°C). The resultant mixture is ethylene glycol dinitrate/nitroglycerin (EGDN/NG). With this development, the freezing hazards of dynamite became a thing of the past in most of North America. Other proportions are also effective, and today economics (the relative prices of the two materials at any given time) generally dictate what the ratio will be. A proportion used by one U.S. company for many years has been 83:17.

Other than the change to the EGDN/NG mixture as a sensitizer, dynamite formulations have changed relatively little since the 1880s when gelatins were invented by Nobel. The notable advances have been in the area of underground coal mining explosives (permissibles) wherein the addition of cooling salts was found to decrease the potential of igniting methane gas or coal dust, and in the introduction of a mixture of metriol trinitrate (C₅H₉N₃O₉; IUPAC name: [2-methyl-3-nitrooxy-2-(nitrooxymethyl)propyl] nitrate) and diethylene glycol dinitrate (MTN/DEGDN) as a non-headache sensitizer substituting for EGDN/NG (Watson and Winston 1985). Dynamites with this new material as a sensitizer found a substantial market in the last quarter of the twentieth century, but are no longer produced. EGDN/NG dynamites are still produced in the United States and elsewhere

Table 1.3 Dynamite Formulations: Generalized (Percent by Weight)

Material	Type ^a				
	1	2	3	4	5
Nitroglycerin	40.0	15.8	91.0	26.0	9.5
Nitrocotton	0.1	0.1	6.0	0.4	0.1
Ammonium nitrate	30.0	63.1		39.0	72.2
Sodium nitrate	18.9	11.9		27.5	
Wood pulp or nut meal	8.0	3.4	0.5	2.0	2.4
Balsa	2.0				
Starch or wheat flour		3.9	1.5	3.8	4.0
Guar gum		1.3			1.3
Microballoons (phenolic)				0.3	
Sodium chloride					10.0
Chalk	1.0	0.5	1.0	1.0	0.5
Total	100.0	100.0	100	100.0	100.0

^a 1, nitroglycerin dynamite (ditching dynamite); 2, 60% extra dynamite; 3, blasting gelatin; 4, 60% extra gelatin; 5, permissible dynamite.

in the world, but in the United States it is produced at only one location (Dyno Nobel, Carthage, Missouri), down from 34 in 1934. Dynamite production in the United States was approximately 30 million pounds in 2006. Some typical formulations are shown in Table 1.3.

1.4.3 Liquid Oxygen Explosives

Dynamite realized some minor competition beginning in the 1920s, when liquid oxygen explosives (LOX) were introduced into the surface coal mines in the central United States. This was a simple material: a cloth cartridge containing carbon black was soaked in a vat of liquid oxygen until the material in the cartridge was totally saturated. The cartridges were immediately lowered into the borehole, stemmed, and shot. A drawback was that only a very limited number of holes could be loaded, since the evaporation of the oxygen was rapid. Even with this limitation, LOX did a good job and were inexpensive. To enhance the economics, mine-site plants were built by oxygen companies. This explosive reached a maximum consumption in the United States of about 25 million pounds in 1953, soon after which, due to developments discussed below, it disappeared from the scene.

1.4.4 Ammonium Nitrate

Ammonium nitrate had been an ingredient in explosives since the earliest days, primarily as an oxidizer in nitroglycerin dynamite mixtures. There had been patents issued wherein the ammonium nitrate was simply mixed with a fuel material, but no significant commercial products resulted.

Since production of the material began, whether for explosives, munitions manufacture, or fertilizer, the physical form of ammonium nitrate was granular: small crystalline particles produced in graining kettles or by other means to slowly dry a highly concentrated liquor. In the mid-1940s, a new, much more economical production method began,

called “prilling.” This method uses the old shot-tower concept used for ages to produce lead shot. With this development, ammonium nitrate became available to the fertilizer trade as a small porous sphere which was free-flowing, absorbent, easily handled and stored, and economical. Ammonium nitrate used as a dynamite ingredient continued (and continues to this day) to be of the granular variety for various reasons of formulation.

1.4.5 Ammonium Nitrate/Fuel Oil

In 1953 a large surface coal mine in Indiana began experimenting with prilled ammonium nitrate and carbon black or ground coal for use as a dynamite or LOX substitute (Hopler 1993a). The efforts were extremely successful and were disclosed to the world by the company, Maumee Collieries, in May 1955. Other mining regions immediately picked up on the benefits of the material, and soon found that fuel oil worked better than the solid fuels. Thus, ammonium nitrate/fuel oil (ANFO) was born. The result was that the entire explosives consuming and producing industries were converted almost overnight from dynamite-based materials to simple fuel/oxidizer mixtures, or *blasting agents*.

A word should be mentioned here about the 1947 disaster at Texas City, Texas, since it is commonly stated that this occurrence brought about the “ANFO revolution.” The disaster involved the detonation of two ships loaded with bags of grained ammonium nitrate fertilizer, with their destination as Europe (Kintz et al. 1948). The probable cause was a fire from smoking by stevedores loading the ship. The ammonium nitrate was rosin-coated for protection against moisture; thus, it was a fueled material, not pure ammonium nitrate. The fact is that it was well known that mixtures of ammonium nitrate and fuel were good explosives, and extensive research had been conducted in the 1930s by explosives companies on such mixtures. They found that these mixtures were relatively insensitive, were easily damaged by the slightest amount of moisture, and would only detonate in relatively large-diameter boreholes.

In 1947, at the time of the Texas City disaster, ammonium nitrate was not yet available in the proper form (prills) for its application as a simple oxidizer/fuel blasting agent. Basically, since it was already common knowledge that ammonium nitrate and fuel worked as an explosive, when the material became available in the prilled form in the 1950s, the mining companies tried it. To state it simply, “the rest is history.” In other words, the ANFO revolution would have happened even if the Texas City disaster had never occurred.

ANFO dominates the commercial blasting industry today, but it is not the perfect explosive. It has no water resistance, has a relatively low density (0.82–0.85 g/mL) and detonation rate (13,000–15,000 f/s or 4000–6000 m/s, dependent on diameter and particle size), and operates rather poorly in small-diameter boreholes unless emplaced in such a way that the particle (prill) size is decreased.

The subject of sensitivity was noted above in relation to the tests with ammonium nitrate–fuel formulations in the 1930s. Blasting agents, one definition of which is that they must fail to detonate when tested with a no. 8 detonator (0.4 g of PETN), are fired in the borehole with a booster explosive in the “explosive train” between the detonator and the blasting agent. The size (weight) of the booster that must be used depends on the blasting agent’s formulation, and can range up to 1 lb. or more of high explosive—usually a cast TNT/PETN mix. In comparison, most “cap-sensitive” emulsion or slurry explosives (Section 1.4.6) require only a no. 8 detonator. Emulsions and slurries can be cap-sensitive or blasting agents, depending on the design. Dynamites, however, are almost universally

cap-sensitive, and many of the more sensitive ones can be initiated with a “fractional” detonator, containing a little as 0.05 g of PETN.

1.4.6 Slurry Explosives

ANFO’s limitations were recognized as soon as the material was introduced, and the first products to evolve in an effort to solve these limitations were the slurry explosives. These were invented in the late 1950s and consisted of ammonium nitrate (usually combined with another oxidizer such as sodium nitrate), water, a gelling agent (usually guar gum), and a high explosive or propellant material for sensitization. Aluminum, in powdered, grained, or flaked forms, was often added for energy. All of the explosives companies were producing slurry prior to 1960. Each company had its favorite sensitizer, usually dictated by patent considerations, success in bidding on war surplus explosives, or the particular in-house expertise of each individual company. The *Encyclopedia* has an excellent compilation of patents in this field (*Encyclopedia*, Vol. 9, S139).

Although all water-based explosives products were called “slurry” in the 1950s and early 1960s, as time passed this product type was subdivided into two distinct classes:

- “Slurry,” which was a thickened (usually by a guar gum, a polysaccharide) but not cross-linked product.
- “Water gel,” which contained a cross-linking agent for the polysaccharide thickeners. The cross-linking agent forms a chemical bond. Early cross-linkers used borate ions, but other materials may be used.

As the surplus sensitizers became more and more difficult to obtain (and more expensive, if available at all), company scientists developed proprietary sensitizers. These included MMAN (monomethylamine nitrate), EGM (ethyleneglycol mononitrate), HMTAN (hexamethylenetetramine nitrate), and MEAN (monoethanol amine nitrate). With these developments, and the frequent use of paint-grade aluminum powders, water gels were able to be manufactured in small diameters to compete in the remaining dynamite markets. However, cost and insensitivity when cold were continuing drawbacks to the water gels. There were many water gels which used only powdered or flaked aluminum for their sensitivity. In the case of flaked aluminum it was shown that the flakes carried air bubbles into the water gel, which provided the sensitive “hot spots” for initiation.

Table 1.4 illustrates some very generalized water gel product formulations. It must be pointed out that there are hundreds of varieties of these products. Even one company’s products will vary greatly depending upon the application, whether packaged (small and large formulas vary) or bulk.

1.4.7 Emulsion Explosives

Almost as soon as the water gels came into usage, another development was made in the commercial explosives field. This new product was the emulsion explosive. Although first conceived in 1961, commercialization was not really successful until the early 1980s.

Whereas water gels/slurries are thickened aqueous solutions of oxidizers and/or fuels and sensitizers/energizers, emulsions are mixtures of two immiscible liquids with one liquid phase dispersed uniformly throughout the second phase. Explosive emulsions are generally “water-in-oil” types, wherein microscopic droplets of the oxidizer phase are

Table 1.4 Water Gels: Examples of Formulations (Percent by Weight)

Material	Formulation					
	1	2	3	4	5	6
Ammonium nitrate	25.3	50.0	40.7	73.8	47.5	42.0
Water	22.5	17.7	13.6	8.9	18.0	15.0
Smokeless powder	25.0					
Sodium nitrate	15.0	15.1	15.8		15.0	
Calcium nitrate						20.0
Hexamine nitrate				14.2		
MEAN						5.0
Sodium perchlorate				2.0		
MMAN			25.9			
Ethylene glycol	1.5	7.2	0.6		1.2	
Diethylene glycol						2.0
Sugar					5.5	
Aluminum	10.0	8.0			12.0	12.0
Gum	0.7	2.0	1.1	1.1	0.8	1.0
Microballoons						1.0
Miscellaneous			2.3			2.0
Total	100.0	100.0	100.0	100.0	100.0	100.0

surrounded by a continuous fuel phase. This provides almost perfect water resistance to the product. Examples of this type of emulsion in the nonexplosive world are butter, margarine, cold cream, and shoe polish.

Emulsion explosives are the ultimate result of the scientific refinement of composite explosives. Black powder, the first composite explosive, had particles that were relatively large. The reaction of the powder, although rapid, was a burning phenomenon on the surface of the particles. Dynamite was the next major composite, with a liquid sensitizer, nitroglycerin, mixed with coarse particles of ammonium nitrate, sodium nitrate, and various carbonaceous materials, examples of which are wood flour, pulp, nut hulls, and sawdust. The chemical reaction of detonation was carried along by the nitroglycerin, but also took place as a surface reaction on the solid materials, as did the burning reaction in black powder, but at shock wave (detonation) velocity rather than at burning velocity. The detonation velocity was adjustable through the choice of particle size of the ingredients.

ANFO, the ammonium nitrate/fuel oil mixture consisting of 94% ammonium nitrate and 6% fuel oil, is probably the most used explosive material in the world today. ANFO is a prime example of a composite explosive, consisting of large particles of ammonium nitrate soaked with oil. Because of the particle size, all of the ammonium nitrate is not in intimate contact with the oil, and thus all of the ammonium nitrate does not react within the detonation reaction zone. This results in ANFO being a less efficient explosive than it should be. An improvement in efficiency, and therefore detonation rate, can be made by reducing the size of the prills. Doing this, however, changes other very important characteristics, such as density, flowability, and certainly not least of all, economics.

In emulsion explosives, the oxidizer portion is drastically reduced in size, thus improving the efficiency of the detonation reaction. Rather than being dry prills, the emulsion oxidizer is a highly concentrated solution of ammonium nitrate and/or other salts. By the

use of emulsifiers and precise processing methods, the “particle size” of droplets of this solution is reduced to microscopic proportions, typically in the range of about 2–10 μm in diameter. Surrounding each droplet is a film of oil, wax, or other fuel material. The result is still a “mixture” of fuel and oxidizer, similar to black powder, dynamite, and ANFO, but the particle size comes as close as possible to mimicking the intimacy of combination found in molecular explosives such as nitroglycerin or TNT.

Emulsions depend upon “hot spots” for their sensitivity. These may be air bubbles resulting from the emulsification process, but they more generally are artificially created by chemical gassing or by the addition of solid “density control” materials such as perlite or microballoons. Microballoons may be of glass or phenolic in a wide range of crushing strengths. A combination of economics and the purpose for which the emulsion will be used dictates the density control type to be used. For example, a ditching application where the explosive may be subjected to high hydrostatic shocks from nearby detonating holes needs an emulsion with high-strength microballoons.

Emulsifier technology is the most important aspect of the competitive situation in the manufacturing industry. The choice of material and the processes used in the emulsion manufacture (temperatures of manufacture, cooling rates, etc.) are important factors in the final explosive, rheological, and shelf-life characteristics of the emulsion. Table 1.5 shows some very generalized emulsion formulas.

Formulation 4 in Table 1.5 was one proposed by the U.S. Bureau of Mines as a permissible explosive (for use in underground coal mines), and is shown only as an example of the diverse collection of materials that may be put into a formulation when economics is not a factor. Commercial companies presently manufacture a great number of emulsions for permissible applications, utilizing formulas closely resembling the others in the table.

The combining of emulsions and ammonium nitrate or ANFO is the latest development in the commercial explosives field. These combinations generally are called “heavy

Table 1.5 Examples of Emulsion Formulas (Percent by Weight)

	1 ^a	2 ^b	3 ^c	4 ^d
Ammonium nitrate	78.0	70.7	58.0	47.0
Sodium nitrate		10.7	15.0	12.0
Water	13.5	7.3	17.0	8.5
Emulsifier	1.5	0.8	2.0	1.5
Oils/waxes	5.5	3.1	6.0	5.0
Aluminum		5.0		
Microballoons	1.5	2.4	2.0	6.0
MMAN				15.0
Sodium perchlorate				5.0
	100.0	100.0	100.0	100.0

Sources: Data from ^{a,b}Sudweeks, W., *Industrial and Engineering Chemistry—Product Research and Development*, 24(3): 432–436, 1985; ^cGehrig, N., In Konya, C.J., *Proceedings of the Eighth Conference on Explosives and Blasting Technique*, pp. 221–228, Cleveland, OH: Society of Explosives Engineers, 1982; ^dRuhe, T. C. and M. S. Wieland, *Proceedings of the Eighth Conference on Explosives and Blasting Research*, p. 70, Cleveland, OH: Society of Explosives Engineers, 1992.

ANFO” or “blends.” The result of this has been to produce a “waterproof ANFO” by having the emulsion material completely coat the dry ammonium nitrate prills or the ANFO. This combination allows loading into wet holes, and in addition enables the explosives engineer to tailor the detonation rate of the material to the rock in question. Emulsions, with their extremely small “particle size” noted earlier, have an inherently high velocity, frequently not suitable for some blasting jobs. The ANFO/emulsion mixtures, however, may be entirely suitable for such situations.

A recent development in the formulation of these blasting agents is the addition of by-product agricultural materials such as seeds or hulls, or other materials such as sawdust, styrofoam beads, coal chips, and so on to lower the density and detonation velocity of the emulsion or emulsion blend (“heavy ANFO”). These bulking agents are of the same types as many of the “dopes” used in dynamites for the past 100 years and more.

The relative insensitivity of ANFO, slurries, water gels, emulsions, and blends, generally requiring a substantial booster for initiation rather than a single detonator (blasting cap), naturally led to their use as bulk-loaded explosives. Hopley (1993b) has written a thorough history of the development of bulk loading.

1.5 Improved or “Do-It-Yourself” Explosives

In recent years the proliferation of various radical movements, some homegrown, some state-sponsored, and others backed by radical fundamentalist movements, have brought with them the illegal use of explosives in misguided efforts to advance their causes. In most cases the explosives have not been those described above, but have been explosives manufactured in clandestine laboratories. Examples of such explosives are urea nitrate, triacetone triperoxide (TATP), and hexamethylenetriperoxidediamine (HMTD). Figures 1.7 and 1.8 show the structural formulae of TATP and HMTD, respectively.

Urea nitrate is prepared from nitric acid and urea. Urea is a widely used fertilizer, and is readily available. Urea nitrate was never used as a commercial explosive because of

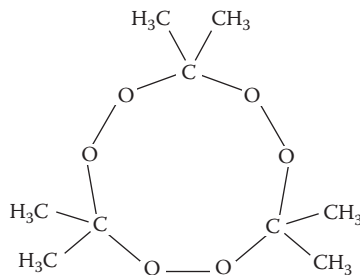


Figure 1.7 Structural formula for TATP.

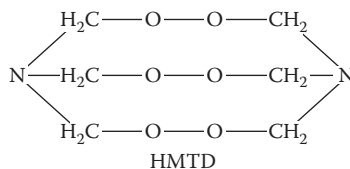


Figure 1.8 Structural formula for HMTD.

its corrosive properties. TATP is a product of the combination of hydrogen peroxide and acetone. In recent years it has become a favorite of terrorists worldwide. It was never a practical commercial explosive. HMTD is a product of hydrogen peroxide and hexamine. It was seriously considered as an initiating explosive at the time when mercury fulminate was the standard base charge in detonators, but never entered serious commercial use. These and other improvised explosives are further discussed in Chapter 12. The precursors of the noted explosives are commercial products. The control of precursor chemicals has been addressed by the National Research Council (1998).

1.6 Methods of Explosives Initiation

With the earliest explosive, black powder (gunpowder), the application of a flame or spark was sufficient to bring about initiation. The insertion of a powder-filled straw sufficed for many years, evolving into the “miner’s squib.” These were dangerous methods, frequently causing the initiation of the main charge before the miner was in a safe position. In 1832 William Bickford invented the safety fuse, which was probably the most significant safety advance in the entire history of explosives.

Upon the discovery of nitroglycerin, it was found that a detonating blasting cap was necessary for successful initiation. This cap could be initiated by a safety fuse, or later, by electrical means. The evolution of electric blasting included bridge-wire and spark gap types, with the bridge-wire being the successful survivor. Delays were built into caps beginning in the early part of the twentieth century, with constant improvement up to the present day. In the twenty-first century, caps (properly called “detonators”) containing computer elements and called electronic detonators are becoming common, with the advantage of extreme accuracy in their timing. Whereas a 1990 detonator was accurate to about 5% of the labeled time at best, the electronic detonator will fire within about 1 millisecond of the designed time.

Advances in the nonelectric detonator field have been spectacular as well. The first nonelectric detonator was a blasting cap crimped onto safety fuse. The next development, in 1903, was the use of a metal tube filled with TNT, which was placed in the borehole along with the main charge. The product was named *cordeau*. Initiation of the tube set off the explosives. Economy and handling were improved in the 1930s by substituting a fabric cover for the metal, and substituting PETN for the TNT. This was called a *detonating cord*. Next, in the 1960s, a delay detonator was attached to a very low-grain core-load detonating cord. In the 1970s, two competing systems were invented, one based on delay detonators attached to empty plastic tubing (*hercudet*), the other based on delay detonators attached to plastic tubing internally coated with a very thin coating of aluminum powder and the explosive HMX (*nonel*). To actuate the first system a mixture of natural gas, hydrogen, and oxygen was introduced by a special blasting machine. When the system was fully charged, a spark initiated a detonation throughout the system of tubes, igniting each detonator. In the second type, a detonation or very strong shock imparted on the aluminum–HMX-coated tubing initiated a dust explosion within the tubing circuit, initiating each detonator, much in the same way as the gas did in the first method. Although both were good systems and had their champions, the aluminum–HMX system prevailed, and the gas system became obsolete. In the early twenty-first century the nonel and electronic detonators appear to be the systems which will dominate commercial blasting for the foreseeable future.

1.7 Summary

The development of emulsions and their applications with ammonium nitrate or ANFO brought about profound changes in the commercial explosives industry. Dynamite is still a viable product, but it is rapidly being displaced in most mining and construction applications. The number of dynamite manufacturing plants (called “works” in the industry) in the United States has gone from 34 in 1934 to just 1 in 2011. In about the same period of time, bulk loading of explosives into the borehole (as opposed to the use of cartridges) has gone from nearly 0 to possibly representing 95% of all commercial explosives usage. This short summary of the vast subject of propellants and explosives may be built upon by the references cited.

References

- Compiled by Tomlinson, W. R. Jr. *Research and Development of Materiel—Engineering Design Handbook*. 1963. Section 1: Properties of explosives of military interest. Washington, DC: U.S. Army Materiel Command.
- Cooper, P. W. and S. R. Kurowski. 1996. *Introduction to the Technology of Explosives*. New York: VCH Publishers, Inc.
- Crowell, B. 1919. *America's Munitions, 1917–1918*. Washington, DC: Government Printing Office.
- Cundill, J. P. 1889. *A Dictionary of Explosives*. Chatham, UK: The Royal Engineers Institute.
- Davis, T. L. 1941, 1943. *The Chemistry and Technology of Explosives*. Vol. 1 and 2. New York: John Wiley & Sons.
- Drinker, H. S. 1878. *Tunneling, Explosive Compounds, and Rock Drills*. New York: John Wiley.
- Encyclopedia of Explosives and Related Items, 1960–1975*. Vol. 1–7. Fedorff, B. T. and O. E. Sheffield. eds. Dover, NJ: Picatinny Arsenal.
- Encyclopedia of Explosives and Related Items, 1978–1983*. Vol. 8–10. Kaye, S. M. ed. Dover, NJ: U.S. Army Research and Development Command.
- Gehrig, N. 1982. The future of slurry explosives. In Konya, C. J. ed. *Proceedings of the Eighth Conference on Explosives and Blasting Technique*, pp. 221–228. Cleveland, OH: Society of Explosives Engineers.
- Hopler, R. B. 1992. Commercial detonators: A review of methods used, past and present, to compare their strengths. *Proceedings of the Eighteenth Annual Conference on Explosives and Blasting Technique*, pp. 191–203. Cleveland, OH: Society of Explosives Engineers.
- Hopler, R. B. 1993a. Custom-designed explosives for surface and underground coal mining. *Mining Engineering* 45(10): 1248–1252.
- Hopler, R. B. 1993b. History of the development and use of bulk loaded explosives, from black powder to emulsions. *Proceedings of the Nineteenth Annual Conference on Explosives and Blasting Technique*, pp. 177–199. Cleveland, OH: Society of Explosives Engineers.
- Hopler, R. B. 1996. The history and development of explosives for underground coal mining. *Proceedings of the Twenty-Second Annual Conference on Explosives and Blasting Technique*, pp. 44–63. Cleveland, OH: Society of Explosives Engineers.
- Kintz, G. M., G. W. Jones, and C. P. Carpenter. 1948. Explosions of ammonium nitrate fertilizer on board the S.S. Grandcamp and S.S. High Flyer at Texas City, Texas, 16, 17 April 1947. R.I. [Reports of Investigations] 4245. Washington, DC: U.S. Bureau of Mines.
- Marshall, A. 1915. *Explosives*. Philadelphia: P. Blakiston's Son & Co.
- Military Explosives*. 1924. Washington, DC: Office of the Chief of Ordnance.
- Munroe, C. E. 1888. Lectures on Chemistry and Explosives Delivered at the Summer Class of Officers of 1888 at the Torpedo Station. Torpedo Station Print.
- National Research Council. 1998. *Containing the Threat from Illegal Bombings*. Washington, DC: National Academy Press.

- Ruhe, T. C. and M. S. Wieland. 1992. Rugged emulsion explosive formulation #37—candidate permissible. *Proceedings of the Eighth Conference on Explosives and Blasting Research*, p. 70. Cleveland, OH: Society of Explosives Engineers.
- Sudweeks, W. 1985. Physical and chemical properties of industrial slurry explosives. *Industrial and Engineering Chemistry—Product Research and Development*. 24(3): 432–436.
- Urbanski, T. 1964. *Chemistry and Technology of Explosives*. Vol. 1. New York: MacMillan. Vol. 2, 3, and 4. Oxford, UK: Pergamon Press.
- Watson, S. C. and S. E. Winston. 1985. A new day for dynamite. In Konya, C. A. ed. *Proceedings of the Eleventh Conference on Explosives and Blasting Technique*, pp. 320–334. Cleveland, OH: Society of Explosives Engineers.
- Williams, W. B. 1920. *History of the Manufacture of Explosives for the World War, 1917–1918*. Washington, DC: U.S. Ordnance Department.
- Wolfe, D. 1991. *Propellant Profiles*. 3rd ed. Prescott, AZ: Wolfe Publishing.

Contents

2.1	Introduction	19
2.2	Historical Developments	20
2.3	Thermochemistry of Explosives	21
2.4	Types of Explosives	23
2.5	Explosion Process	24
2.5.1	Pressure of an Explosion	24
2.5.2	Energy Release in Explosions	25
2.5.2.1	Oxygen Balance	26
2.5.3	Detonation Properties	27
2.6	Characteristics of Blast Waves	28
2.6.1	Reflection of Blast Waves	32
2.6.2	Scaling and TNT equivalency	36
2.6.2.1	Scaling	36
2.6.2.2	TNT equivalency	37
2.7	Types of Hazards	38
2.7.1	Missile Impact on Concrete	41
2.8	Interaction of Blast Wave with Structures	42
2.8.1	Calculation of Blast Load	43
2.8.2	Blast-Resistant Structures	44
2.8.3	Hazards to Personnel	46
2.8.4	Blast Protection	49
2.9	Conclusion	50
	References	52

2.1 Introduction

The instantaneous release of energy from a relatively small volume of material can be viewed as an explosive event. This is achieved by changes in the chemical composition of the solid, liquid, or gas, and the release of chemical energy. Depending on initiation conditions, charge geometry, and chemical composition, this reaction can accelerate until a steady value (detonation) has been achieved, or decelerate (deflagration) and eventually die out. The distinction between true detonation and deflagration is not crucial at this stage, as both processes can lead to release of very large amounts of energy in a small fraction of a second. Most incidents involving dust or vapor cloud explosions (flour, sawdust, gasoline vapors, natural gas, etc.) involve only rapid combustion and not detonation. Most commercial explosives such as ammonium nitrate (AN)-fuel oil mixtures exhibit nonideal behavior, in that their sensitivity and severity of explosion falls off rapidly with decreasing diameter and lack of confinement. In this discussion, confined to condensed

phase explosions, the words “detonation” and “explosion” are used synonymously and no distinction is made between commercial and military explosives.

The whole subject of explosion hazard has gained great immediacy in recent years, partly because of widespread terrorist activity employing explosives and the measures required to protect people and property against such actions, and partly due to increasing emphasis on social and environmental concerns regarding their manufacture, transport, storage, and use, especially in urban areas. Since the basic reaction chemistry of an explosive compound is somewhat straightforward, and some of the ingredients required to produce such products are often in regular household use, it becomes increasingly difficult to control and track these supplies. This applies particularly to regular use of improvised explosive devices among many trouble spots around the world, where the makers of such devices do not need to worry about their long-term stability, toxicity, or cost, all of which play a major role in the manufacture of explosive products for strictly civilian and military use. It therefore becomes imperative that the explosion process itself is fully understood and appropriate protective measures are implemented to prevent loss of life and damage to structures, and to suitably address environmental issues.

The energy from an open-air explosion results in compression of the surrounding air, which gives rise to a rapidly propagating shock wave or pressure wave. Except in the immediate vicinity of the explosion, where the explosion fireball may pose a serious hazard, the major hazards resulting from an accidental explosion are due to the shock wave and high-velocity fragments expanding from the explosion site. The medium of transmission could be air, water, or soil and rock. The main characteristic of the shock wave is an extremely sharp rise in pressure value in the front, followed by a slow decay. The front part of the wave is entirely compressive and the tail part of it is entirely tensile but of much lesser amplitude. The amplitude of the compressive shock in the immediate vicinity of this explosion could be in excess of 10 GPa (or a hundred thousand atmospheres); it decreases very rapidly, however, as it travels away from the source of the explosion. The velocity of shock would depend on the stiffness of the medium in which it travels, and it is normally a constant in each medium for relatively low-amplitude shock pressures. However, its amplitude and duration (both of which contribute to its damage potential) can be altered dramatically through multiple reflections caused by proximity of the explosion to ground surface or other free or rigid structures. This can result in significant increase in the amplitude of the “reflected” shock compared to the “incident” shock.

The additional hazards resulting from an explosion include the explosion fireball, secondary fragments, cratering, perforation, and spalling. The effect of the shock wave on personnel and structures has been studied extensively in recent years, and guidelines established for its damage potential. There are currently several excellent monographs and treatises available on the subject of science and technology of explosives. There are also comprehensive design handbooks dealing with blast hazards and blast-resistant structures. The purpose of this paper is not so much to summarize these available sources of information but to provide an up-to-date review of the interrelated topics and elucidate the scope and complexity of the subject.

2.2 Historical Developments

It is difficult to speak of modern explosives without referring to black powder. The discovery of black powder probably precedes its actual use in a systematic fashion by several centuries. Its essential ingredients (potassium nitrate, charcoal, and sulphur) have been available

since ancient times, and chance or deliberate ignition of a mixture of these ingredients may not have been so rare. However, the credit for its systematic use belongs to the Chinese, who packed these mixtures into bamboo tubes and used them as rockets for display and signaling purposes. It took several centuries before black powder became a standard military tool. Even then, the early fourteenth century cannons consisted simply of wooden tubes filled with black powder charge which expelled a stone projectile. The first use of the material in mining took place in Hungary in the early seventeenth century. Its use accelerated with the discovery of vast deposits of sodium nitrate in Chile in 1840.

Other related developments quickly followed. In 1846, strong nitric acid reacting with glycerol, a by-product of soap manufacture, resulted in an oily product called glyceryl trinitrate, which is more commonly known as nitroglycerin (NG). Practical use of NG was pioneered by the Nobel family in the years following 1859. Alfred Nobel also invented the blasting cap in 1863, which revolutionized the mining industry. But the behavior of the NG-based explosives still remained highly unpredictable, resulting in numerous accidents and fatalities. After many years of work, Nobel finally discovered that kieselguhr, a diatomaceous earth, absorbed up to three times its own weight of NG to form a relatively dry, leak-resistant paste, which came to be known as “dynamite” (Meyers and Shanley 1990). The word was derived from “dynamis,” the Greek word for “power.”

Other momentous advances in the explosives technology include the development of safety fuse (essentially a black powder core inside a tough yarn) by William Bickford in 1831, the invention of the detonating cord (a sensitive high explosive core inside a thin plastic tube or textile yarn) in 1908 in France, the further refinement of the detonating cord by Ensign-Bickford Corporation in the United States, and the chance discovery of AN as a very powerful explosive in 1947, when the ship *Grand Camp* carrying fertilizer-grade AN blew up at its dock in Texas City following a fire. The place of AN in explosives industry has since been secure. The other significant developments in the explosive industry were the introduction of the slurry explosives in the late 1950s and shock tube-based detonators (“nonel”—a plastic tube with a wall coating of high melting explosive [HMX] and aluminum) in the early 1970s, water-in-oil emulsion explosives in the late 1970s, and accurate electronic delay detonators in the 1990s.

2.3 Thermochemistry of Explosives

Explosive reactions can be slow or fast, the former characterized by low rates of reaction (a few centimetres to a few m/s) and the latter by very high rates (up to several km/s). The reactivity of a chemical depends on its chemical structure. All explosive chemicals such as nitrate ($-\text{ONO}_2$), nitro ($-\text{NO}_2$), chlorate (ClO_3^{-1}), and perchlorate (ClO_4^{-1}) are characterized by low thermodynamic stability.

The chemical compositions of typical molecular explosives are shown in Figure 2.1. The oxygen attached to these structures breaks away easily to combine with other elements such as carbon, hydrogen, sulphur, and so on to form more stable compounds. There are also some explosive compounds which are either highly oxygen-deficient (e.g., trinitrotoluene [TNT]) or totally devoid of it (e.g., lead azide [PbN_3]). However, it can be said that in general, most explosives contain carbon (C), hydrogen (H), nitrogen (N), and oxygen (O), and are categorized as “C-H-N-O” explosives.

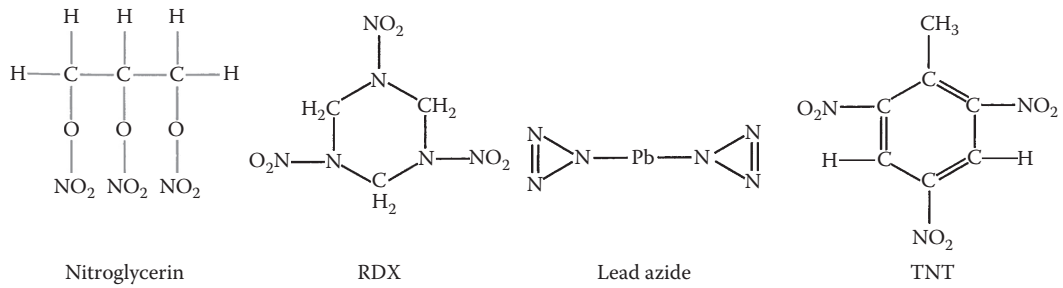
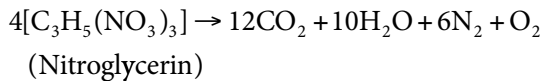
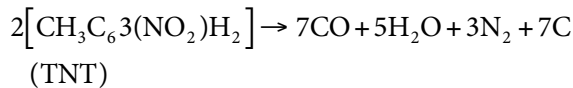
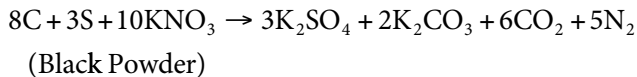


Figure 2.1 Chemical composition of typical molecular explosives.

The major reactions in the explosion process are the following: C to carbon dioxide, H to steam and water, N to nitrogen gas, aluminum (Al) to aluminum oxide, sulfur (S) to gas or solid sulphates, AN to water, nitrogen, and oxygen, and so on. The following rules of thumb can be applied to determine the reaction hierarchy: all nitrogen forms N₂, all hydrogen converts to H₂O, any excess oxygen converts to CO, any further oxygen left combines to form CO₂ and Al₂O₃, with balance remaining O₂, and any excess C remains solid carbon. On this basis, let us examine the reaction process in three classical explosives: black powder, TNT, and NG.



In each case, the unstable union between nitrogen and oxygen is transformed into more stable compounds; nitrogen reuniting with itself, oxygen combining with carbon, hydrogen, and sulphur. Actual reactions at the high temperatures and pressures prevailing in the reaction zone are, of course, more complex, and the relative gas fractions continually change as the temperature inside the explosion drops.

All explosive compounds can be considered to be composed of three components: fuel, oxidizer, and sensitizer. Thus, any number of these ingredients in combination can be combined to form an explosive mixture, the main difference among them being their respective energy content, sensitivity, and stability. Carbon, hydrogen, sulphur, and so on provide the essential fuel for the oxygen in the oxidizer. Incorporation of a chemical or physical sensitizer enhances the ease with which the explosive can be made to react by means of an initiator. The molecular explosive compositions already contain the necessary ingredients within them, without the requirement for additional fuel additives. Most of these molecular explosives, such as NG or TNT, do not require a sensitizer, whereas others may require such components in order to attain a degree of sensitivity that is practical from a blasting point of view. A partial list of sensitizers is given in Table 2.1.

Table 2.1 Typical Sensitizers in Commercial Explosives

Chemical	Physical
Composition B TNT	Aluminum (fine)
RDX Monoethylamine Nitrate	Air bubbles
Nitroglycerin Perchlorates	Glass or plastic microballoons
Nitromethane Nitropropane	

The bulk of the commercial explosives are not molecular explosives but are made of mixtures of these three essential components. As a result, they are considerably less sensitive (and therefore safer and cheaper) than the molecular explosives (e.g., PETN [pentaerythritol tetranitrate], TNT, NG, etc.). Initiation of these explosives is therefore much more difficult, and requires adequate boosting. The common form of initiators and boosters are detonators (~1 g of PETN), detonating cords (4 g/m to 40 g/m of PETN), cast boosters (20 g to 1 kg of pentolite [PETN/TNT 50/50]), and cartridged explosives (200 g to 500 g of detonator-sensitive commercial explosives).

2.4 Types of Explosives

Explosion events could originate from several sources. These include dust explosions, ignition of flammable gases and initiation of condensed phase chemicals such as propellants and explosives, and finally, detonation of nuclear devices. Dust and vapor cloud explosions are the most common form of accidental events and are discussed in Chapter 7. The basic mechanics of damage is similar to that due to chemical explosives, so the present discussion will deal only with the latter.

Chemical explosives can be roughly grouped under two categories: military explosives and commercial explosives. There is, however, no sharp distinction except in their applications and their relative sensitivity to initiation. Military explosives, as well as the so-called primary explosives used in the manufacture of detonators, are normally composed of molecular explosives which require no additional ingredients to make them explode. Examples include lead azide, lead styphnate, TNT, PETN, RDX (research department explosive), and various combinations of the latter three compositions such as semtex (RDX/PETN). In general, the molecular explosives have higher sensitivity and higher reaction rates than composite explosives. Despite their extensive military use and apparent familiarity, most of these explosives were developed only during the early half of the twentieth century.

The development of commercial explosives preceded military explosives by several decades and continues to be an active area of research. Examples include NG-based explosives (dynamites), explosives with alternate sensitizers such as TNT, RDX, and perchlorates, slurry explosives, emulsions and dry blasting agents such as ANFO (ammonium nitrate and fuel oil). All explosives other than NG-based ones may contain varying amount of aluminum for extra energy. Although NG-based and slurry explosives still have a significant market share, dry blasting agents such as ANFO and emulsion explosives and their variants have become the mainstay of most commercial blasting operations in all civil and mining projects.

The emulsion explosives have several outstanding advantages over other explosives including their simplified composition (saturated AN liquor with fuel oil and an appropriate emulsifier), intimate mixing of fuel and oxidizer (droplet size ranging from 1 μm to 5 μm), relative resistance to water, ease of manufacture, and high velocity of detonation. Emulsion explosives can be sensitized, for small diameter applications, with either chemical or physical sensitizers (air bubbles or glass or plastic microballoons), and can incorporate varying amounts of aluminum to give them additional strength. They can be manufactured in a wide range of densities—lower densities for small-diameter application and higher densities for large-diameter application. The emulsion explosive can be used by itself or mixed with ANFO or AN prills, or it can be used as a filler of intergranular spaces in ANFO. The bulk of the commercial explosives in use today are either straight ANFO or its derivatives with emulsions, either in bulk form or in cartridge form. However, commercial explosives can also be manufactured in a variety of other forms, such as castings, pressings, putties, and rubberized and plastic bonded forms for specialized applications.

2.5 Explosion Process

Heating a reactive material results in its exothermic decomposition. The resulting heat may further increase the rate of reaction and may eventually lead to a self-sustained reaction known as “deflagration.” A rapidly traveling shock wave also can provide the initial source of heat in the material. Under certain conditions of initiation and confinement the deflagrating reaction can transit to a supersonic but steady rate of reaction, otherwise known as “detonation.” In deflagration mode, the reacted materials flow away from the unreacted material, whereas in detonation mode, the detonation products flow with great velocity toward the undetonated explosive.

In the detonation process, a shock front or shock zone propagates at a characteristic velocity into the unreacted explosive at very high pressures and temperatures. Immediately behind the shock front is the chemical reaction zone, where the original material is rapidly converted into reaction products. The width of the shock front and the reaction zone could be as low as a few millimeters depending on the nature of the explosive material and the boundary conditions. The chemical reaction zone is followed by a slower-moving zone consisting of the detonation products. The mechanism is shown schematically in Figure 2.2. The pressure and temperature in the detonation zone could exceed several hundred thousand atmospheres and 3000°C.

2.5.1 Pressure of an Explosion

One can get some idea of the magnitude of the pressure associated with an explosion process by treating the gaseous explosion products as ideal gases. The ideal gas law is given by

$$PV = nRT$$

where P is the pressure, V is the volume, n is the moles of gas, R is the gas constant, and T is the absolute temperature.

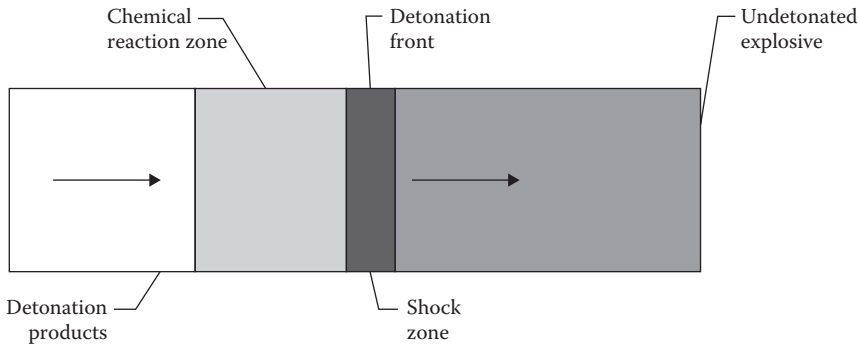


Figure 2.2 Simplified structure of detonation reaction in an explosive mixture.

Table 2.2 Pressure–Volume Relationship per Mole of Gas at 0°C

Pressure (atm)	Hydrogen		Oxygen		Carbon Dioxide	
	<i>V</i>	<i>PV</i>	<i>V</i>	<i>PV</i>	<i>V</i>	<i>PV</i>
1	22.428	22.43	22.393	22.39	22.262	22.26
100	0.2386	23.86	0.2075	20.75	0.04450	4.45
400	0.07163	28.65	0.05887	23.55	0.04051	16.21
800	0.04392	35.13	0.04207	33.66	0.03779	30.23
1000	0.03837	38.37	0.03886	38.86	0.03687	36.87

Source: Data from Manon, J. J., *Engineering and Mining Journal*, 177: 60–68, 1976.

Table 2.3 Some Equations of State to Relate Pressure–Volume–Temperature Relationship

Name	Relationship ^a
van der Waals	$(P + a / V^2)(V - b) = 2$
Becker-Kistiakowsky-Wilson (BKW)	$PV = RT(1 + \chi e^{\beta\chi}); \chi = (\kappa \sum X_i k_i) / [V/T + \theta]^\alpha$
Beattie-Bridgman	$PV^2 = RT[V + B_0(1 - b/V)][1 - c/V T^3] - A_0(1 - a/V)$

^a *P, V, T, R, X, and k* denote pressure, volume, temperature, gas constant, species mole fractions, and individual species volumes. As expected only *R* is a constant in the above equations, and the fitting parameters *a, b, c, A₀, B₀, C₀* and $\alpha, \beta, \theta,$ and κ must be determined from experimental data.

This pressure–volume–temperature relationship holds only at relatively low pressures at which molecules of gas are relatively far apart. However, under explosion reaction conditions this is far from so, as seen in Table 2.2 for three representative gases. Real gases are seen to be much more compressible, as the varying values of *PV* indicate.

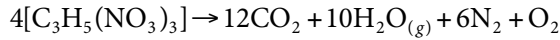
To account for the behavior of gases at temperatures and pressures characteristic of the explosion process, several “equations of state” (EOS) have been proposed with varying degrees of success. Some typical examples of these are shown in Table 2.3.

2.5.2 Energy Release in Explosions

In simple terms, the amount of heat released can be taken to be the equivalent of the energy content in an explosive. In its simplest form, the heat released in a detonation reaction is

the difference between the heat of formation of the original reactants and those of its reaction products. By convention, the heat of formation of all elements in the standard state (25°C and 1 atmosphere) is taken to be zero. Thus the known heat of formation of compounds can be used to predict the heat of detonation. The detonation of NG can be taken as an example:

$$H_{p(\text{explosion})} = H_{p(\text{products})} - H_{p(\text{explosive})}$$



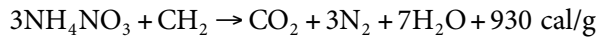
$$- H_p = 12(94) + 10(58) - 4(83)$$

$$= 367 \text{ kcal/g} - \text{mole at } 0^\circ\text{C}$$

$$\text{or } 1620 \text{ cal/g}$$

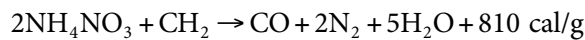
The energy released in ANFO can be similarly calculated. A simple calculation goes as follows:

$$94.5\% \text{ AN} + 5.5\% \text{ FO}$$



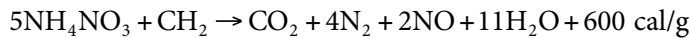
For slightly different proportions of AN to fuel oil, the results would be as follows:

$$92\% \text{ AN} + 8\% \text{ FO}$$



and

$$96.6\% + 3.4 \text{ FO}$$



Clearly the maximum amount of energy is released with a 94.5:5.5 ratio of ANFO.

The energy calculations shown above apply to the "ideal" energy release; the actual energy release and the associated detonation parameters (e.g., reaction temperature, detonation pressure and its decay, detonation velocity, etc.) will depend on the density, confinement, diameter, and initiation mode of the explosive in question.

2.5.2.1 Oxygen Balance

The role of oxygen is crucial in optimizing the reaction products for maximum release of heat. As shown above, with few exceptions most molecular explosives are oxygen-deficient.

To achieve full oxidation it is necessary to add oxygen-rich ingredients in making explosive mixtures with these explosives. The ratio of oxygen present to the amount of oxygen required to achieve full oxidation is a measure of the oxygen balance. As the above equations show, ANFO with 8% fuel oil is oxygen-negative or has a negative oxygen balance as evidenced by the presence of CO in the reaction products. Similarly, lowering the fuel oil to 3.4% renders the ANFO oxygen-positive with extra oxygen being in the form of NO in the reaction products. Most commercial explosive compositions are formulated ideally to have a zero oxygen balance.

2.5.3 Detonation Properties

Conservation of momentum across the shock front results in rapid acceleration of the reacted material in the direction of shock. This is termed the *particle velocity*. The density, pressure, particle velocity, and temperature in the reaction zone must all obey conservation laws of physics. The Chapman–Jouget (C–J) postulate states that the sound velocity in the reacted material plus the particle velocity must be at least the same as the shock wave velocity, to ensure that the chemical reaction energy can be transported forward to sustain the shock front. The C–J plane defines the limit beyond which no further energy release can contribute to the propagation of the shock front. The corresponding pressure is known as the C–J pressure. These characteristic pressures for some typical explosives are shown in Table 2.4, along with their density and velocity of detonation.

Besides density, the other critical parameter controlling detonation properties is the charge size or charge diameter. This applies particularly to the more insensitive commercial explosives, where the velocity of detonation is not only a strong function of charge diameter, but such explosives are not detonable below a certain critical diameter. For commercial explosives, the critical diameter ranges from 20 mm to 200 mm depending on the density and composition. The other distinguishing features of commercial explosives are their generally lower density and lower velocity of detonation and pressure. However, despite their somewhat reduced hazard potential in terms of damage to structures and injury to personnel, detonation of commercial explosives, deliberate or otherwise, still represents an extremely serious hazard.

Table 2.4 Detonation Parameters of Some Typical Explosives

Explosive	Density (g/cm ³)	Detonation Velocity (m/s)	Detonation Pressure (GPa)
ANFO	0.84	4500 ^b	4.3
Slurry	1.25	4800 ^b	7.2
Emulsion	1.20	5500 ^b	9.1
Dynamite	1.45	5400 ^b	10.6
TNT ^a	1.64	6930	21.0
PETN ^a	1.67	8000	30.0
RDX ^a	1.77	8700	33.8

^a Data from Dobratz, B. M. and P. C. Crawford, *LLNL Explosives Handbook: Properties of Chemical Explosives and Explosive Simulants*, Livermore, CA: Lawrence Livermore National Laboratory, University of California, 1985.

^b Maximum value—actual figure will depend on diameter and confinement.

2.6 Characteristics of Blast Waves

The original potential energy in the explosive upon detonation is distributed among a number of distinct forms as a function of space and time. These consist of

- Wave energy
- Residual or waste energy
- Kinetic and potential energy of confining material or fragments
- Kinetic energy of source material
- Source potential energy
- Radiation

The energy distribution is shown schematically in Figure 2.3. The energy in a propagating wave system is both potential and kinetic, but excludes that contained in the volume occupied by the explosion products or the quiescent medium between the blast wave and the products (Strehlow and Baker 1976). Thus, at far field, the total wave energy—a characteristic of each explosive type—should remain constant with time. The residual or waste energy represents the heat generation in the intervening air due to passage of the shock wave, which is irreversible.

The kinetic and the potential energy imparted to any confining medium or resulting fragments due to the initial expansion of the shock wave can be a significant fraction of the total energy. This is done through plastic deformation, heat transfer, and so on. Similarly, some amount of energy is also transferred as kinetic energy to the explosive source material. All kinetic energy components must eventually reduce to zero as the fragments or the source materials come to rest. In a typical explosion process, a considerable amount of energy is still retained by the explosion gases, which are still under relatively high pressures

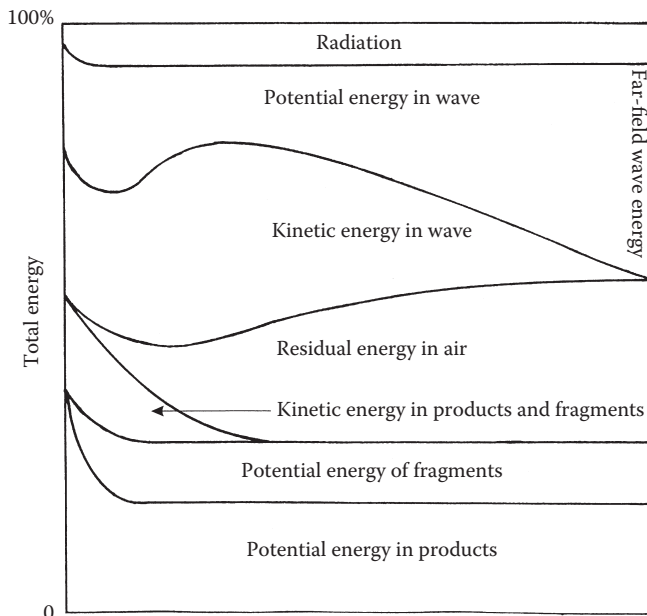


Figure 2.3 Energy distribution (schematic) in an explosion event as a function of time.

and temperatures. This is known as the *potential energy* of the product. Although this energy is eventually dissipated through expansion and cooling, the time scale in which this occurs is much larger than that associated with the propagation of the blast wave.

The final component of energy loss is represented by radiative heat losses. However, this is rather a small fraction of the total heat energy in chemical explosions compared to nuclear explosions. Figure 2.3 shows that only a fraction of the total available explosive energy appears as wave energy. A larger fraction of the total energy, however, may be transferred to the blast wave in the case of a slower rate of release of explosive energy.

The characteristic propagation and decay of blast wave in air is shown schematically in Figure 2.4a. With greater time (or larger distance travelled), the blast wave undergoes systematic changes in amplitude, duration, and profile. In the far field, the pressure signature assumes a pronounced negative phase. Figure 2.4b shows the features of an ideal blast pressure profile and its relevant features. This should be compared with an actual pressure profile recorded from a 6.4 kg (14 lb) near-surface ANFO charge at a distance of 2.1 m (7 ft), as illustrated in Figure 2.4c.

The similarity between the ideal shock pressure profile and that from measurement is remarkable. The leading part of the blast wave is compressive with an extremely rapid rise in pressure level, which is followed by exponential decay of the pressure. Due to the inertial effect, the pressure eventually falls below the atmospheric level and then returns more or less to the ambient level after some time. The amplitude of the negative phase of the blast wave is only a fraction of the positive phase, although in the far-field conditions its duration is larger than the positive or the compressive phase. Initially, the velocity of the blast wave, due to the high pressures involved, could be several thousand m/s, but with distance the shock decays to a regular sound wave in air with the characteristic velocity of ~330 m/s. From this it is evident that the shock wave from a larger or more intense explosion will arrive at a given site sooner than due to a weaker explosion.

A very important aspect of the shock wave in air is the high velocity wind associated with the shock front. The pressure resulting from the latter is called the dynamic pressure (Kinney 1962). It is proportional to the square of the wind velocity and to the density of the air mass behind the shock front. It can be shown that the dynamic pressure becomes larger than the peak overpressure when the latter reaches or exceeds 480 kPa (70 psi). The calculated peak dynamic pressure and the corresponding wind velocity are shown in Table 2.5.

Since the dynamic pressure denoted by q is proportional to the square of the wind velocity (u) and the density (ρ) of the shocked air, it can be written as

$$q = 1/2(\rho u^2)$$

which is essentially the kinetic energy per unit volume of air immediately behind the shock front. It can be further shown that

$$q = P_s^2 / [2\gamma P_0 + (\gamma - 1)P_s]$$

which, for $\gamma = 1.4$ (the ratio of the specific heats at constant pressure and at constant volume for air) reduces to

$$q = 5/2 P_s^2 / (7 P_0 + P_s)$$

where P_0 is the ambient pressure and P_s the peak overpressure. The above expression will be used in calculating the reflected overpressure to be discussed in the next section.

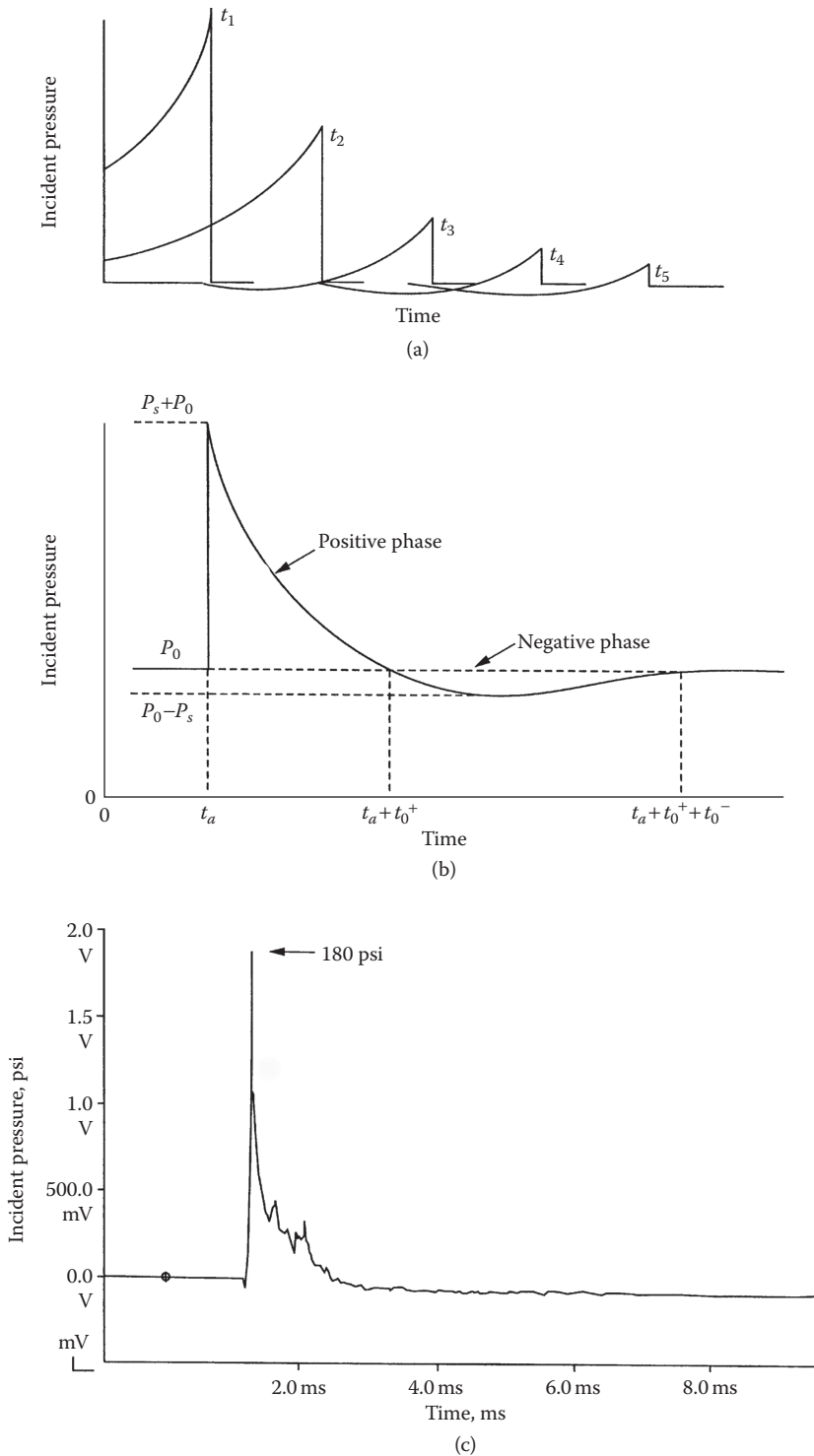


Figure 2.4 (a) Idealized propagation and decay of the shock wave from an explosion at increasing distances; (b) a typical shock pressure profile; (c) a measured shock profile from a small near-surface ANFO charge 6.4 kg (14 lb) at a distance of 2.1 m (7 ft) from the source.

Table 2.5 Peak Overpressure, Dynamic Pressure, and Maximum Wind Velocity in Air at Sea Level for an Ideal Shock Front

Peak Incident Pressure kPa (psi)	Peak Dynamic Pressure kPa (psi)	Max. Wind Velocity km/h (mph)
345 (50)	283 (41)	1531 (934)
207 (30)	117 (17)	1097 (669)
69 (10)	15.2 (2.2)	482 (294)
34.5 (5)	3.7 (0.5)	253 (154)
20.7 (3)	1.4 (0.2)	162 (99)
13.8 (1)	0.7 (0.1)	115 (70)

Source: Adapted from Glasstone, S. and P. J. Dolan, *The Effects of Nuclear Weapons*, 3rd ed., Washington, DC: U.S. Department of Defense, 1977.

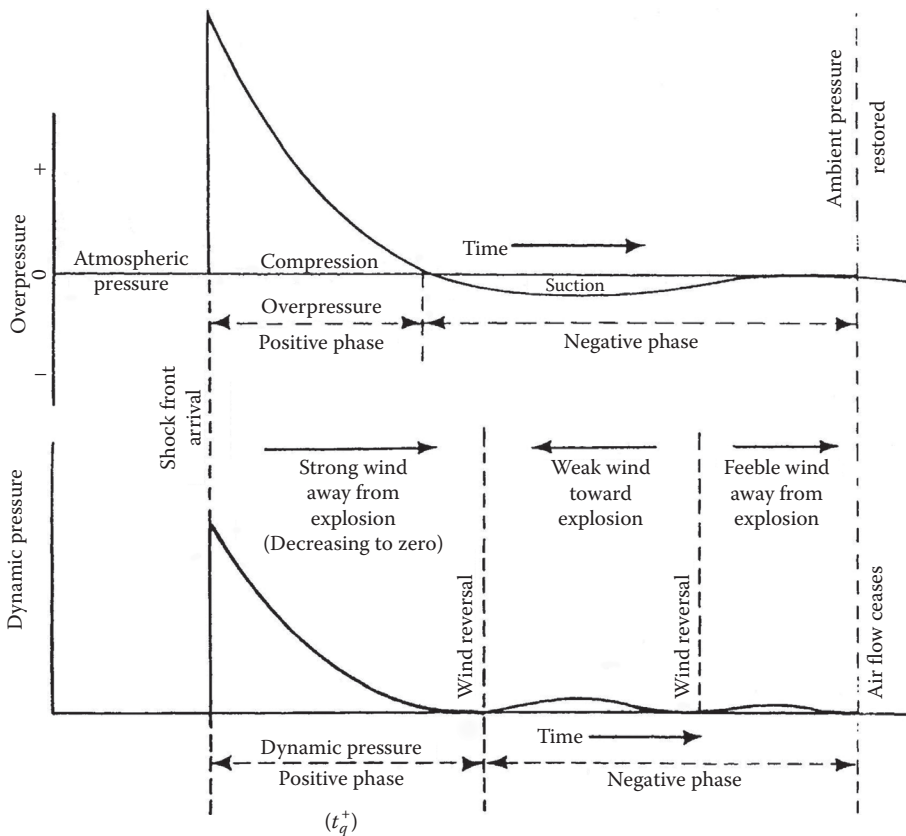


Figure 2.5 Shock pressure profile from a free-air explosion and the associated dynamic pressure at a fixed distance from the explosion. (Adapted from Glasstone, S. and P. J. Dolan, *The Effects of Nuclear Weapons*, 3rd ed., Washington, DC: U.S. Department of Defense, 1977.)

The peak dynamic pressure and its duration play a critical role in the development of the drag force around a structure and the ensuing damage. The relationship between the shock pressure and the dynamic pressure is illustrated more graphically in Figure 2.5.

As expected, there is a small time lag, due to inertial effects, between when the shock and the dynamic pressure reach the atmospheric pressure. Also, unlike the shock, the

dynamic pressure is never negative. Initially, the blast wind blows away from the explosion, but when the shock pressure goes below ambient, the wind direction reverses and it now flows, albeit at a much lower velocity toward the source of the explosion. Although the dynamic pressure has a longer duration than the shock pressure, it is of relatively low amplitude in the latter part and does not pose a significant hazard to a target. It can also be shown that it decays faster than the direct shock pressure.

2.6.1 Reflection of Blast Waves

When a shock wave impinges on a “rigid” target, be it the ground surface or a building, it undergoes reflection and possibly diffraction. Assumption of a rigid target makes the analysis simpler at this stage, as it precludes any significant energy transfer through refraction or deformation of the target. Also for simplicity, only “grazing” or normal incidence at right angles to the target is considered in this analysis. When a spherical explosive charge is detonated sufficiently far away from the ground surface or any other reflecting surface, the shock pressure expands spherically, and its characteristics such as peak, duration impulse, and arrival time, at a certain location, are known as *free-air* explosion parameters. This is in contrast to *surface* explosion parameters where the explosive charge is near or on the ground surface.

The explosion parameters are very different for these two conditions. In the former case, any point above the ground surface would experience two distinct shocks: one due to the incident or direct shock from the explosion and the other a reflected shock from the ground surface (or any other reflecting surface). The latter would be delayed with respect to the direct shock because of the extra travel path involved. The explosion resting on the ground would produce only a single shock, but it will have significantly different characteristics than the *free-air* burst, especially in its peak amplitude.

A free-air spherical explosion upon reflection from the ground surface also gives rise to an important modification to the shock profile. As the reflected shock has to travel in preshocked air (caused by the direct shock), it travels at higher velocities than its own amplitude would demand. This eventually leads the reflected shock to merge with the direct shock, forming what is known as a triple point (Figure 2.6). The region between ground surface and the triple point is called the Mach region, and the corresponding shock front is known as the Mach stem. Both the height and the peak value of the Mach stem have a critical bearing on blast loading of structures. For the surface burst, there will no region of reflection, but the amplitude of the shock would be considerably higher than the

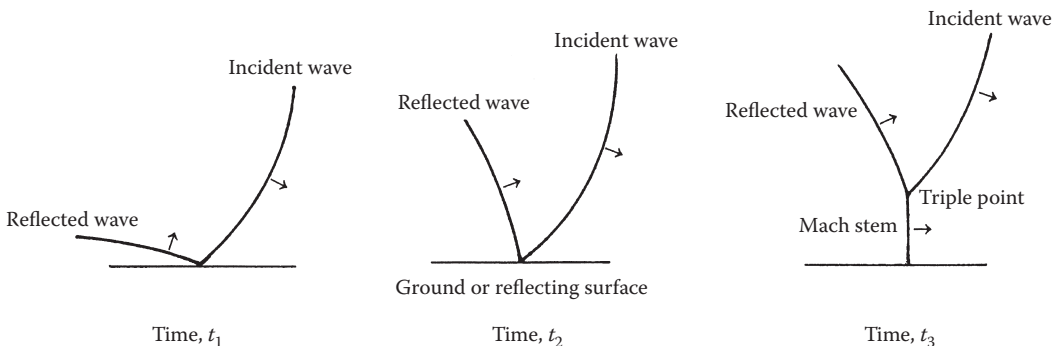


Figure 2.6 Formation of the triple point and Mach stem upon reflection of a shock wave.

free-air case. In fact, it would be the same as in the Mach stem, with the blast wind blowing more or less horizontally close to the ground surface.

Regardless of whether the explosion is a free-air or a surface burst event, when the shock wave impinges on a rigid target it undergoes reflection and diffraction, the extent of the latter depending very much on the shape and size of the target. The pressure in the shock wave impinging on a target is known as the “incident” or “side-on” pressure (P_s), which upon reflection from a target is known as the “reflected” pressure (P_r). There are additional complications for oblique impacts, so only the case of normal incidence for a plane shock (i.e., shock front parallel to a flat-faced target) is considered here. It can be shown that for such a case, the instantaneous reflected pressure, P_r , is given by

$$P_r = 2P_s + (\gamma + 1)q$$

Upon using the penultimate equation and assuming $\gamma = 1.4$ for air, the above reduces to

$$P_r = 2P_s(7P_0 + 4P_s)/(7P_0 + P_s)$$

This shows that for very strong shocks (i.e., $P_s \gg P_0$), the instantaneous “reflected” pressure can be eight times that of the “incident” shock pressure at normal incidence. Conversely, for weak shocks (i.e., $P_s \approx P_0$), the reflected pressure is only twice that of the incident pressure, which is the simple acoustic case. Baker (1973), however, has suggested that the relationship $P_r = 8 P_s$ for strong shocks is an oversimplification since it is based on the assumption that the air behaves like an ideal gas at such high temperatures and pressures. The maximum value of the reflected shock in reality could be much higher than this. It is evident however from the above equation that the reason for the reflected pressure being greater than $2P_s$ is due to the presence of the dynamic pressure associated with the blast wind discussed earlier.

The free-air measurement of the blast wave parameters forms much of the basis for estimation of explosion hazards. A very large number of tests have been performed over decades involving mostly spherical TNT and pentolite explosive charges. By means of the principles of scaling and equivalency, to be discussed in Section 2.6.2, the blast parameters for other explosives can be calculated for various quantities and at various distances.

Typical shock wave data for a free-air spherical TNT explosion are shown in Figure 2.7 as a function of “scaled distance.” The latter is defined as the ratio of distance over the cube-root of the weight of explosive ($x/w^{1/3}$). The parameters shown are for the positive phase only. These include the peak incident and reflected pressure (P_s and P_r), the corresponding impulses (i_s and i_r), the arrival times (t_a), the duration of the positive phase (t_0), and the wave length (L_w). Similar curves can be generated also for the negative phase of the blast wave. The common practice is to represent them in scaled terms (i.e., scaled with respect to the cube-root of the charge weight), so that shock wave parameters can be obtained for any combination of charge weight and distance. It is clearly evident that the reflected pressure is many times higher than the incident pressure even at relatively low incident pressures (~10 psi). One has to be almost at a scaled distance of 50 away (i.e., 50 ft from a 1 lb charge or 15 m from a 0.5 kg charge), or 500 ft from a 1000 lb charge (i.e., 150 m from a 455 kg charge) before the reflected pressure becomes sufficiently small and the blast wave can be considered an ordinary acoustic wave.

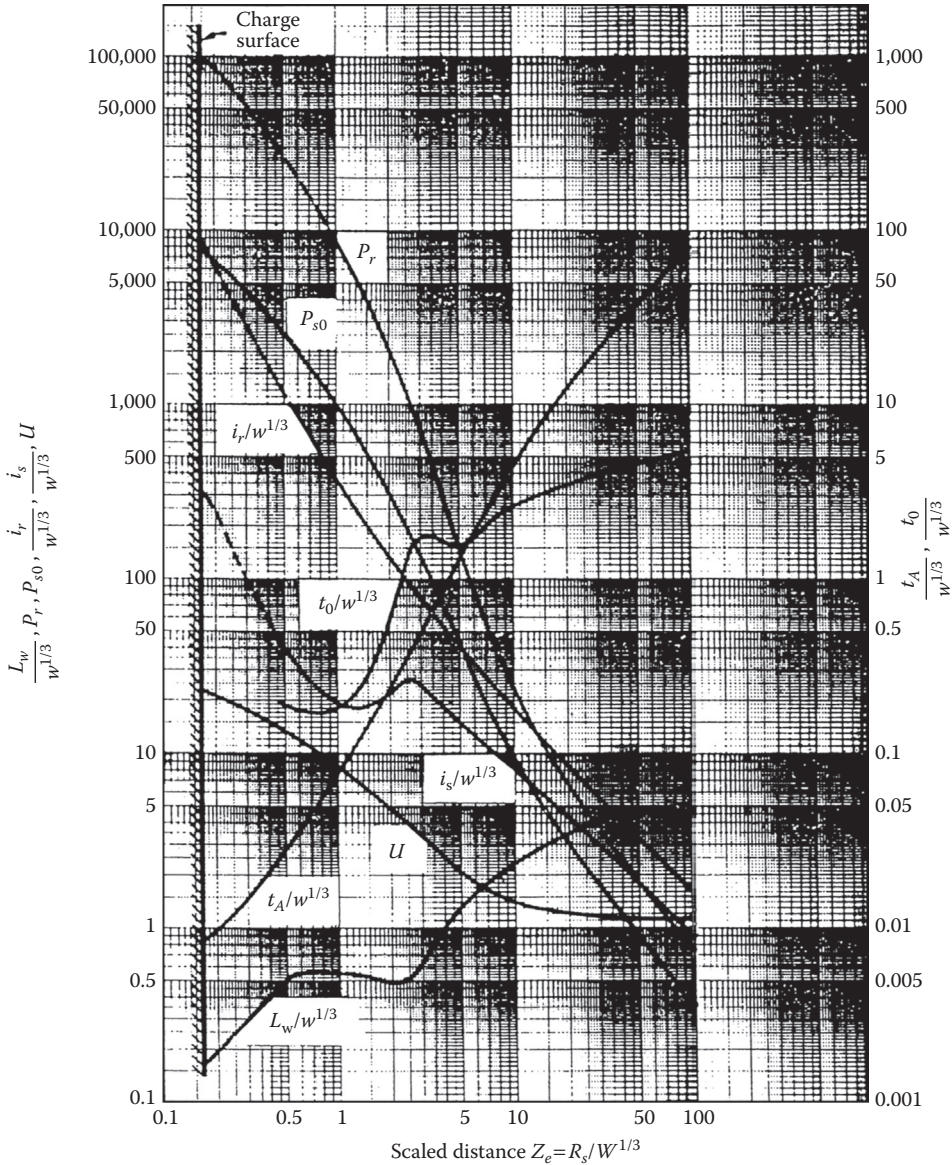


Figure 2.7 Shock wave parameters (positive phase only) for a free-air spherical TNT explosion at sea level. (Adapted from Joint Departments of the Army, Navy, and Air Force, *Structures to Resist the Effects of Accidental Explosions*, Washington, DC: U.S. Government Printing Office, 1990.)

The shock parameters shown in Figure 2.7 change significantly for a surface or near-surface burst. The same applies when the charge shape deviates from spherical symmetry. Three such examples for hemispherical, spherical, and cylindrical charge of Composition B (RDX/TNT/wax ratio of 56:40:4) are shown in Figure 2.8 for surface explosions. The variation of both incident pressure and impulse with shape is clearly evident at identical scaled distances. Similar variations occur with more common shapes such as hoppers, bags, or flat beds of explosives, but values for these can normally be extrapolated from the above three cases.

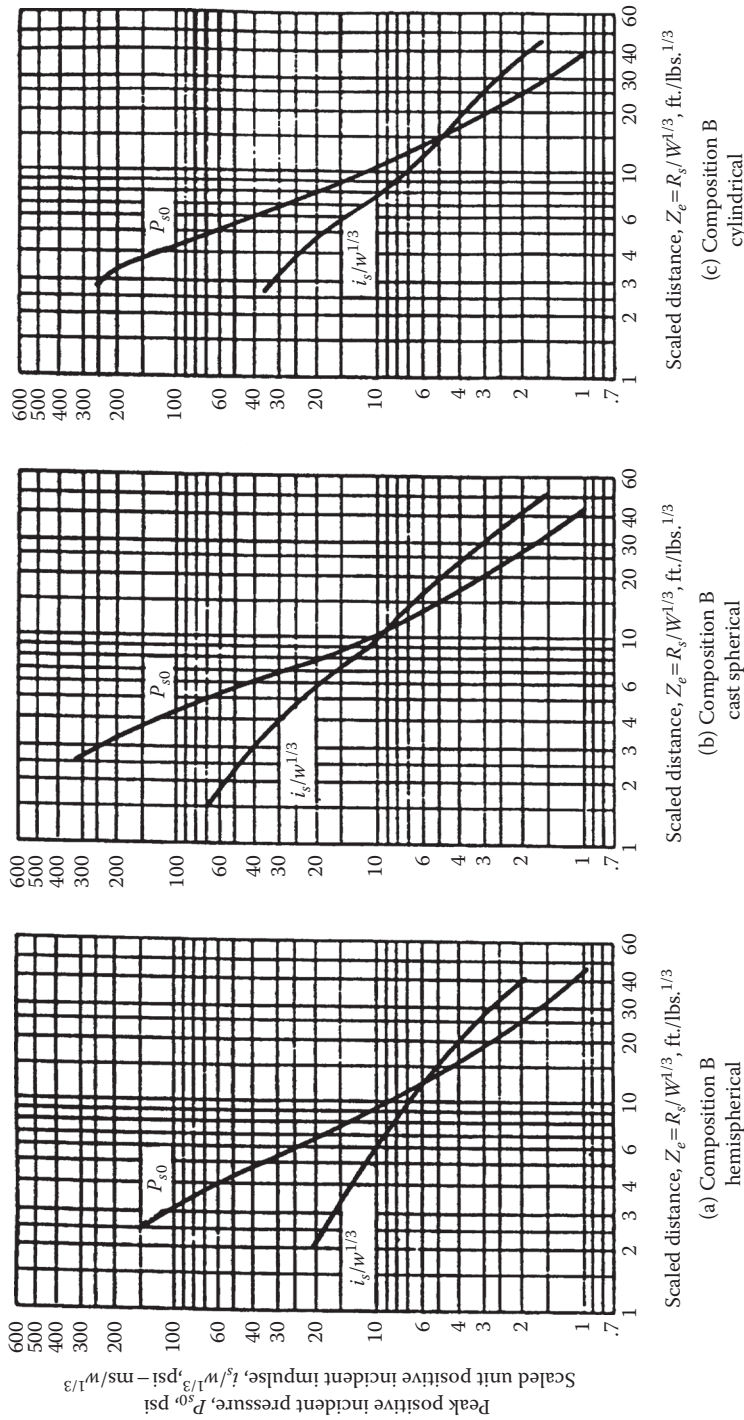


Figure 2.8 Changes in shock wave parameters due to change in shape of the explosive source for Composition B. (Adapted from Joint Departments of the Army, Navy, and Air Force, *Structures to Resist the Effects of Accidental Explosions*, Washington, DC: U.S. Government Printing Office, 1990.)

2.6.2 Scaling and TNT Equivalency

An accidental explosion can involve a variety of conditions, such as specific types of explosives, charge geometry, height of burst, and atmospheric pressure conditions. Since the source conditions in most accidents are not known very accurately, estimation of the size of the explosion or the incident blast overpressure for assessing damage (or designing against damage) would be a formidable task. To overcome this, the techniques of “scaling” and “TNT equivalency” are widely used to estimate the size of an accidental explosion or design blast-resistant structures. This allows calculation of blast parameters from different explosive-distance combinations from standard tables of such parameters available for TNT and pentolite (see Figure 2.7).

2.6.2.1 Scaling

The self-similarity of air shock from detonation of a variety of explosive types was mentioned in Section 2.6.1. The most common practice of explosion scaling is based on “cube root” scaling, otherwise known as Hopkinson’s law (Baker 1973). It states that for any pressure generated at a distance R_1 from a reference explosion of W_1 , in weight, the same pressure would be registered at a distance R_2 from a different explosive of W_2 in weight, provided

$$R_2/R_1 = (W_2/W_1)^{1/3}$$

Similar relationships apply to time (t) and impulse (I):

$$t_2/t_1 = R_2/R_1 = (W_2/W_1)^{1/3}$$

$$I_2/I_1 = R_2/R_1 = (W_2/W_1)^{1/3}$$

The above equation means that two different weights of the same explosive would give the same pressure at the same “scaled distance” (i.e., $z = \text{distance}/(\text{charge weight})^{1/3}$). Similarly, an observer stationed at a distance λR from the center of an explosive charge with characteristic dimension λd would experience a similar blast wave with amplitude P , duration λt , and impulse λI , to a reference explosive having the characteristic dimension d and the same pressure, P . Hopkinson’s law has been shown to hold true for a variety of explosives and energy yields.

The conditions described above apply to similar types of explosives, spherical charge geometry, and identical atmospheric conditions during detonation. Except for the latter, these can be easily controlled or duplicated. Another scaling law, known as Sachs’s scaling law, is applied to correct for changes in the atmospheric conditions. The corresponding multipliers to pressure, distance, time, and impulse (S_p , S_d , S_t , and S_i respectively) based on Sachs’s law are given below:

$$S_p = (P_a/P_0)$$

$$S_d = (W_2)^{1/3}/S_p^{1/3}$$

$$S_t = (W_2)^{1/3}/S_p^{1/3} \cdot (288/T_a + 273)^{1/2}$$

$$S_i = (W_2)^{1/3}/S_p^{2/3} \cdot (288/T_a + 273)^{1/2}$$

where, P_a is the ambient pressure, P_0 the standard sea level atmospheric pressure (14.7 psi or 101.3 kPa), and T_a the ambient temperature in °C.

The equations and the conditions described above apply strictly to spherical or nearly spherical charges, whereas most real explosions involve nonspherical charge geometrics. With an asymmetrical explosive source, the azimuthal variation of shock wave parameters becomes very significant. A considerable body of experimental and empirical data exists to correct for the effect of asymmetry and generate equivalent spherical charges, which can then be used with the standard TNT blast parameter charts (Baker et al. 1980). However, caution must be exercised in any extrapolation of available data to a subject explosion whose geometry and orientation are known only approximately. A good example of this is represented by explosions in confined spaces such as tunnels, where both the peak pressure and its duration can be affected significantly when compared to free-air detonations. In carefully controlled experiments in a 3 m × 3 m mine tunnel, it has been shown that the incident peak shock pressure from an unconfined explosive charge at a distance of 21 m inside the tunnel can be more than an order of magnitude larger than a similar detonation in open air. The corresponding impulse could be more than two orders of magnitude larger than measured for a free-air surface detonation (von Rosen and Guilbeault 2008). The increased amplitude, especially the measured impulse is the result of multiple reflections along the walls of the tunnel. The measured values of shock will also differ depending on the roughness of the tunnel wall, tunnel dimension, and the presence of any reflecting surface behind the explosive charge.

2.6.2.2 TNT Equivalency

Since extensive experimental data exist for TNT explosions, it is customary to find a “TNT equivalency” for a subject explosive, and then use only the TNT blast parameters to assess or predict damage, design appropriate blast-resistant structures, or station personnel. The two approaches for estimating TNT equivalence are: (1) by calculation, and (2) by experiment.

The former is based on the calculated energy equivalence between TNT and the subject explosive. This is based on the calculated heats of explosion and assumes that the detonation reaction is an ideal one and all the energy calculated is actually released. The alternative method is to arrive at the equivalency from specific structural damage studies and relate it to known damage levels from specified overpressures. This approach can, however, lead to large errors because the degree of damage, such as collapse of walls or breakage of windows, cannot be accurately correlated with the levels of overpressure. The best approach is through actual measurement of shock pressure parameters (pressure and impulse) followed by comparison to standard charts of the equivalent weight of TNT, which would yield the same pressure or impulse at the same distance. The equivalency can be expressed as

$$N_p = (W_{\text{TNT}}/W) = (Z/Z_{\text{TNT}})^3 P_s = \text{constant}$$

$$N_i = (W_{\text{TNT}}/W) = (Z/Z_{\text{TNT}})^3 i_s = \text{constant}$$

where W is the weight of the subject explosive, z is the scaled distance (distance/weight^{1/3}), and N_p and N_i represent equivalency based on the incident pressure and incident impulse respectively.

Table 2.6 Comparison of TNT Equivalency by Different Methods for Selected Explosives

Explosive	TNT Equivalency		
	Pressure	Impulse	Calculated Energy
TNT	1.0	1.0	1.00
Composition B	1.2	1.3	1.09
Pentolite	1.5	1.0	1.09
PBX-9404	1.7	2.0	1.11

Source: Adapted from Esparza, E. D., *Proceedings of the 22nd Department Defense Safety Seminar, 26–28 August 1986*. Alexandria, VA: Department of Defence, Explosives Safety Board, 1986.

Note: For incident pressure range of 100–1000 psig, corresponding to scaled distance range of 3.5 to 0.74 ft/lb^{1/3} with spherical charges.

Unfortunately, the calculation method and the two experimental methods (pressure and impulse) do not always yield the same TNT equivalency (Esparza 1986). A comparison among the three approaches is shown in Table 2.6. Note also that the standard pressure and impulse curves for TNT are based on a spherical or hemispherical charge, whereas any deviation from this geometry can give rise to very different shock pressure profile and its duration (Held 1983, 1999). The same caution has to be exercised in obtaining TNT equivalency for gas or vapor cloud explosions (Trelat et al. 2007).

As the data show there is considerable discrepancy among the three methods. On the experimental side, there is usually much greater uncertainty in the measurement of impulse than peak pressure. Equivalency based on the peak incident pressure is therefore the preferred method, but structures designed to resist impulse load would require the use of TNT equivalency based on impulse.

The calculation of equivalency based on standard TNT curves yields reliable results for high explosives exhibiting ideal or near-ideal detonation behavior. It is much more difficult to arrive at similar equivalency figures for the nonideal detonations characteristic of some of the commercial explosives. These may exhibit relatively long run-up distances before they achieve steady detonation velocity, or there may be significant reaction behind the C–J plane due to granularity or inhomogeneity of the explosive matrix. The same applies to other types of explosions such as pressurized bursting vessels, dust, and vapor cloud explosions. The calculated energies from the latter types is normally much higher than actually released because the calculations must assume optimum dispersion of oxidizer and fuel elements in the dust or vapor cloud—a situation which rarely exists in practice. These types of explosions usually have lower peak pressures of much longer duration, and their damage potential is significantly different than those due to condensed phase explosives.

2.7 Types of Hazards

The severity of hazards from a deliberate or accidental explosion depends on a number of factors. The quantification of a hazard would depend on the target as well as the medium of shock transmission. Increased environmental concerns now require protection of aquatic life against underwater shock from normal underwater blasting activities, for example seismic exploration, underwater demolition, and so on. The mitigative

criteria in such cases are based on amplitude and duration of shock as well as the weight and type of fish involved, as well as the target's proximity to surface of water (Keevin and Hempen 1997). Different considerations apply if one is seeking the protection of structures rather than people. Even here, one has to define the degree of protection sought; for example, minor structural damage may be acceptable but not injury to people. The hazard could result from any number of factors such as air shock, ground cratering, seismic vibrations, collapse of buildings, fragments and missiles, ground ejecta, and explosion fireballs and thermal radiation. Of these, cratering and fireballs do not pose a serious hazard as they are confined to the immediate vicinity of the explosion. Thermal radiation is not a major factor in chemical explosions. Seismic vibrations caused by ground shock can result in some damage to structures located at a considerable distance from the site of the explosion, but at these distances the damage is minor and does not pose a threat to people.

It is nevertheless possible to estimate the crater dimensions from knowledge of the ground conditions and the fireball dimensions from knowledge of the explosive composition and its detonation characteristics. Thus, in terms of severity, air shock and fragment and missile hazards pose the most serious threat to both structures and personnel in an explosion. The interaction of shock waves with structures and the nature of biological hazards will be described in greater detail in Section 2.8.3. However, the pressure resistance values shown in Table 2.7 for various structural elements, which were first published four decades ago, provide a good starting point. Various national standards are currently in force for protection against accidental explosions during manufacture, storage, and transport of explosives. These Q-D (quantity-distance) regulations are based on extensive documented data from the world wars, as well as accidental explosions and some controlled tests. These regulations essentially follow the NATO guidelines on the subject of protection

Table 2.7 Conditions of Failure of Peak Overpressure-Sensitive Elements

Structural Element	Failure	Approximate Incident Pressure kPa (psi)
Glass windows, large and small	Shattering, occasional frame failure	3.5–6.9 (0.5–1)
Corrugated asbestos siding	Shattering	6.9–13.8 (1–2)
Corrugated steel or aluminum paneling	Connection failure followed by buckling	6.9–13.8 (1–2)
Wood siding panels, standard house construction	Usually failure occurs at the main connections, allowing a whole panel to be blown in	6.9–13.8 (1–2)
Concrete or cinder block wall panels 8–12 in thick (unreinforced)	Shattering of the wall	13.8–20.7 (2–3)
Self-framing steel panel building	Collapse	20.7–27.6 (3–4)
Oil storage tanks	Rupture	20.7–27.6 (3–4)
Wooden utility poles	Snapping failure	34.5 (5)
Loaded rail cars	Overturning	48.3 (7)
Brick wall panel 8–12 in thick (unreinforced)	Shearing and flexure failures	48.3–55.2 (7–8)

Source: Adapted from Brasie, W. C. and D. W. Simpson, *Proceedings of the Symposium on Loss Prevention in the Process Industries, 63rd National Meeting AIChE*, St Louis, MO, New York: Association of Industrial Chemical Engineers, 1968.

from explosion effects, and the criterion employed is simply incident shock pressure versus quantity of explosives (or its TNT equivalence) involved (NATO 2006; NRCAN 1995). The calculated distance restrictions for a variety of structures and situations provide a very large degree of protection against the effect of accidental explosions. However, these guidelines are not aimed at the design of specific structures for blast resistance.

As will be shown in Section 2.8, the response of a structure depends usually on a combination of peak pressure and impulse (i.e., integral of pressure–time profile), and it is quite likely that different structures at the same site would have to be designed to withstand an impulse load rather than peak pressure load and vice versa. The figures in Table 2.7 do show the easy fragility of even solid structures when exposed to relatively low-level blast overpressures.

The fragment and missile hazards represent a different and very difficult problem in terms of their quantification and prediction. These also include ground ejecta from surface bursts, as well as spalling of material due to an intense shock impacting on the opposite face of a structural member or machinery. A large amount of experimental data is available that tries to relate fragment characteristics (i.e., size, distribution, and velocity) with the amount of explosive involved in the detonation. These studies have been carried out, of necessity, with simple geometries with both contact and decoupled charges. The basis for all predictions is tied to the Gurney energy constant, which is defined as a characteristic fragment velocity specific to each explosive. It has been experimentally determined that, at least for simple geometrical configurations in mild steel, the initial velocity (V_0) of a metal fragment can be related to the weight of the explosive and the metal casing by

$$V_0 = (2E')^{1/2} f(W, W_c)$$

where V_0 is the initial velocity, $(2E')^{1/2}$ is the Gurney energy constant, W is the weight of explosive, and W_c is the weight of steel casing. Examples of the Gurney energy constant (in ft/s) for several explosives are shown in Table 2.8.

For a cylindrical container weighing W_c (lb) and filled with explosive weighing W , the last equation takes the form

$$V_0 = (2E')^{1/2} [(W/W_c)/(1 + W/(2W_c))]^{1/2}$$

For a thin-walled cylinder and an explosive mass much larger than that of casing, the maximum initial velocity becomes

$$v_{\max} = 1.41(2E')^{1/2}$$

Table 2.8 Gurney Energy Constant $(2E')^{1/2}$ for Selected Explosives

Explosive Type	Density (g/cm ³)	$(2E')^{1/2}$ (ft/s)
Composition B	1.72	9100
PBX-9404	1.84	9500
PETN	1.76	9600
RDX	1.77	9600
TNT	1.63	8000
Nitromethane	1.14	7900
Tritonal	1.72	7600

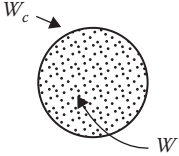
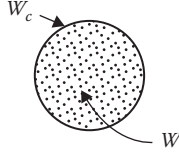
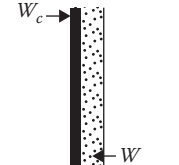
Type	Cross-sectional shape	Initial fragment velocity v_0	Maximum v_0
Cylinder		$\sqrt{2E'} \left[\frac{\frac{W}{W_c}}{1 + \frac{W}{2W_c}} \right]^{1/2}$	$\sqrt{2E'} \cdot \sqrt{2}$
Sphere		$\sqrt{2E'} \left[\frac{\frac{W}{W_c}}{1 + \frac{3W}{5W_c}} \right]^{1/2}$	$\sqrt{2E'} \cdot \sqrt[5]{3}$
Plate		$\sqrt{2E'} \left[\frac{\frac{3W}{5W_c}}{1 + \frac{W}{5W_c} + \frac{4W_c}{5W}} \right]^{1/2}$	$\sqrt{2E'} \cdot \sqrt{3}$

Figure 2.9 Gurney energy relations for calculation of fragment velocity for simple geometries.

The Gurney energy relations for other simple geometrics are summarized in Figure 2.9. The velocity of a fragment will depend on its mass, its shape, and the distance traveled from the explosive source. Initial velocities can be calculated for different combinations of container geometry and explosive weight and type for specific fragment mass. The assumption of a certain fragment shape and use of the appropriate drag coefficient can also yield a velocity profile over distance for specific fragment mass. Considerable analytical and experimental work has been carried out to estimate fragment size as well as mass distribution from exploding steel casings (Joint Departments of the Army, Navy, and Air Force 1990; Cooper 1996; Koch et al. 2002), which can be combined with velocity information to arrive at critical impact parameters which a specific target must be designed to withstand.

Despite the wealth of information available, the calculation of fragment size and velocities is still extremely difficult except for the simplest geometrics and mild steel casings. Although the more complex but common types of containers or parts of machinery can be broken down to individual cylindrical or spherical components, the calculated values must be used with a great deal of caution. The primary fragments issuing from an exploding vessel or container can also give rise to secondary fragments upon impact against other structural elements or machinery parts. Prediction of the characteristics of these secondary fragments or missiles is generally much more uncertain. However, once the missile characteristics have been defined, the response of structural or biological targets to their impact is more easily handled. The response of human targets will be discussed in a Section 2.8.3. They are more vulnerable to both primary and secondary fragments.

2.7.1 Missile Impact on Concrete

A steel fragment impacting on a concrete target can simply bounce back with a reduced velocity, or, with sufficient initial velocity, can cause perforation and spalling of the target.

The rate of penetration of the missile depends on its mass and striking velocity. Initially the only effect on the concrete target surface is the formation of a crater due to dislodgement of material at the point of contact. As the velocity increases to 300 m/s (1000 ft/s) or more, the fragment usually penetrates beyond the bottom of the crater. This may be accompanied by spalling of concrete on the rear side of the target. The velocity of spalled fragments can be high enough to cause injury or lead to sympathetic detonation of explosive material stored beyond the concrete wall. With sufficient striking velocity the fragment can penetrate the target and may eventually lead to perforation of the concrete wall. Empirical design equations have been obtained from experimental programs on concrete perforation, and these can be used with reasonable accuracy, provided the velocity and mass of the striking fragment are known. Based on these relations, it is predicted, for example, that a 4 in (10 cm) diameter fragment travelling at 3000 ft/s (900 m/s) will easily perforate a 12 in (30 cm) thick concrete wall.

2.8 Interaction of Blast Wave with Structures

The pressure exerted by the shock front on a target is known as the shock load, where all the phenomena discussed earlier (reflection, diffraction, dynamic pressure, etc.) may become operative. Except for explosions at great heights, all surface or near-surface events have pronounced or exclusively horizontal forces. The three types of loading that occur in this interaction with a target are compression loading, diffraction loading, and drag loading. The relative significance of these various loading conditions depends on the amplitude and duration of the shock wave, and also on the type of construction, the geometry of the structure, and its orientation with respect to the shock front. When the explosion occurs at considerable height above a relatively low-rise structure, the shock load initially is all compressive and almost simultaneous on all parts of the structure. In contrast, the loading characteristics from a surface or near-surface explosion are more complex.

When a steep shock front impacts on the face of a structure, it undergoes reflection with the resulting pressure buildup on the face being at least twice that of the incident pressure. However, for a structure of finite dimensions, the incident pressure wave continues on in the original direction of propagation and eventually engulfs the entire structure. This is known as *diffraction loading*. For a relatively small structure with little or no openings, diffraction loading results in compression of the entire structure by about the same pressure, as contained in the incident overpressure. However, for a larger structure and a near-surface explosion, the diffraction effect would lead to differential loading of the front section of a structural member (e.g., roof or side-wall) compared to its rear section. The resulting relative displacement of a structural member during diffraction of the shock wave can have the same or greater damage potential than when the wave has finally engulfed the entire structure. Diffraction loading will continue until the positive phase of the shock has finally traversed the length of the structure and the pressure has fallen to ambient level. The presence of openings such as doors and windows or the collapse of any structural member during the diffraction process would lead to lower pressures and rapid equalization of pressure within and outside the structure. The resulting pressure rise in the interior of the structure is known as the *leakage pressure*.

When the shock wave impacts on a structure, there is also an additional load due to the dynamic pressure caused by the strong winds behind the shock front. This is known

as *drag loading*, which has a longer duration than the positive phase of the incident shock. For an explosion source with a long positive duration phase, the structure could be subjected to drag loading for a significantly longer duration than due to diffraction. In case of a tower with open lattice or truss members such as electric pylons, the expected pressure differential will vanish rapidly, as the incident pressure will go round these slender structural members that make up the tower, and the pressure will equilibrate within a fraction of a millisecond. In such cases, it is the particle velocity u and the positive duration of the pressure pulse and not the shock velocity U or the incident overpressure P_i that will define the damage. The particle velocity u is a direct measure of the dynamic pressure associated with the blast wave (i.e., the peak wind velocity behind the shock front) (see Section 2.6). Large buildings in general will respond mainly to the latter, whereas columnar structures such as smokestacks, electric transmission towers, and truss bridges respond mainly to drag forces. On the other hand, large buildings with substantial openings or with weak sides or roofs that collapse soon after the arrival of the shock become drag-type structures. The drag loading of a structure depends on shock wave parameters (amplitude and duration) as well as on the shape of the structure. The influence of this shape factor on the drag coefficient is less for streamlined objects (grain silos, smokestacks) than for irregular or box-like structures. The actual pressure generated is a product of the drag coefficient and the calculated value of dynamic pressure from the blast winds. Also, since the duration of the shock is proportional to the energy yield or size of an explosion for the same threshold overpressure, a high-yield explosion would cause more extensive damage at the same scaled distance than a low-yield one.

2.8.1 Calculation of Blast Load

The response of a structure would vary considerably, depending on whether the explosion is external or internal. In the case of the former, the structure would be designed to mostly resist pressure, whereas for the latter it would be designed to mostly resist impulse. When an external blast pressure impacts on the outside of structure (e.g., the front wall of a box-like structure with little or no opening, and a shock front moving perpendicular to the plane of the wall), the pressure is immediately amplified to assume the value of the reflected pressure, P_r . However, this decays rapidly to what is known as the stagnation pressure, P_{st} , which is the sum of the incident overpressure P_s and the dynamic pressure times the appropriate drag coefficient for the structural element. For the simple case considered (normal impact with $P_s < 50$ psi), the drag coefficient is unity, and the time, t_s , it takes the pressure to reduce to P_{st} is $3 S/U$, where S is equal to the height of the wall or its half-width, whichever is less, and U is the shock velocity. The stagnation pressure is thus

$$P_{st} = P(t_s) + C_p q(t_s)$$

where q is the dynamic pressure and C_p is the drag coefficient. Beyond t_s , the pressure decays to the ambient pressure, the total duration being equal to that of the positive phase of the incident overpressure. The blast loading profile for this example is shown in Figure 2.10. Similar profiles can be worked out for the roof and the side and rear walls.

For an internal explosion, the pressures are normally much higher and the duration shorter. In this case, the impulse loads on the walls and the roof would have to be calculated. Based on extensive experimental studies, a scheme has been worked out to calculate the impulse loads for specific geometrics of a cubicle and explosive locations (Joint